

# Multi-field effects in a simple extension of $R^2$ inflation

Taro Mori,<sup>a</sup> Kazunori Kohri<sup>a,b</sup> and Jonathan White<sup>b</sup>

<sup>a</sup>SOKENDAI (The Graduate University for Advanced Studies), Oho 1-1, Tsukuba 305-0801, Ibaraki, Japan

<sup>b</sup>Theory Center, IPNS, KEK, Oho 1-1, Tsukuba 305-0801, Ibaraki, Japan

E-mail: [moritaro@post.kek.jp](mailto:moritaro@post.kek.jp), [kohri@post.kek.jp](mailto:kohri@post.kek.jp), [jwhite@post.kek.jp](mailto:jwhite@post.kek.jp)

**Abstract.** We consider inflation in the system containing a Ricci scalar squared term and a canonical scalar field with quadratic mass term. In the Einstein frame this model takes the form of a two-field inflation model with a curved field space, and under the slow-roll approximation contains four free parameters corresponding to the masses of the two fields and their initial positions. We investigate how the inflationary dynamics and predictions for the primordial curvature perturbation depend on these four parameters. Our analysis is based on the  $\delta N$  formalism, which allows us to determine predictions for the non-Gaussianity of the curvature perturbation as well as for quantities relating to its power spectrum. Depending on the choice of parameters, we find predictions that range from those of  $R^2$  inflation to those of quadratic chaotic inflation, with the non-Gaussianity of the curvature perturbation always remaining small. Using our results we are able to put constraints on the masses of the two fields.

---

## Contents

<b>1</b>	<b>Introduction</b>	<b>1</b>
<b>2</b>	<b>Set-up and background equations</b>	<b>2</b>
<b>3</b>	<b><math>\zeta</math> and its correlation functions using the <math>\delta N</math> formalism</b>	<b>5</b>
<b>4</b>	<b>Numerical analysis and results</b>	<b>11</b>
<b>5</b>	<b>Summary</b>	<b>21</b>

---

## 1 Introduction

Recent cosmic microwave background (CMB) observations are in good agreement with the predictions of inflation, and the data is now so precise that it can be used to constrain individual models of inflation [1]. While observations are still perfectly consistent with single-field inflation, in the context of high-energy particle physics theories there is strong motivation to consider multi-field models. For instance, when compactifying superstring theory or supergravity on to four dimensions, many scalar/pseudo-scalar fields usually appear, such as moduli and axions. It is thus important to determine the observable consequences of multi-field inflation models and how they, and the theories in which they are embedded, can be constrained by current and future observations. In relation to this there are perhaps two key features that distinguish multi-field models from single field models. The first is that the curvature perturbation on constant density slices,  $\zeta$ , is not necessarily conserved on super-horizon scales, and the second is that its statistical distribution may deviate from a Gaussian one. In the case of single-field inflation, Maldacena’s consistency relation dictates that the non-Gaussianity of  $\zeta$  in the squeezed limit should be unobservably small, which is a consequence of the fact that  $\zeta$  is conserved on super-horizon scales in single-field inflation models [2]. This suggests that if a relatively large non-Gaussianity were to be observed, this would be a strong indication that multiple fields were present during inflation. Even if not observed, however, it is still important to determine the implications of this for multi-field models. While current constraints on non-Gaussianity from the CMB are relatively weak, future large scale structure surveys promise to improve these constraints considerably, see e.g. [3]. In light of the above, it is clear that in looking to test any multi-field model of inflation one will need to be able to calculate how the curvature perturbation evolves on super-horizon scales and how much its statistical distribution deviates from a Gaussian one.

In this work we consider a simple multi-field extension of so-called  $R^2$  inflation, also sometimes referred to as Starobinsky inflation [4]. In its Jordan frame representation, the original model consists of a modified gravity sector containing a term proportional to  $R^2$ , and the inflationary predictions are in very good agreement with observations [1]. In trying to embed this model in a more fundamental framework such as a supergravity, however, it is natural to expect the appearance of additional scalar degrees of freedom (see e.g. [5]) and an important question is then how much the inflationary predictions are affected by these additional degrees of freedom. As a toy model, here we consider adding a canonical scalar field with quadratic mass term to the original Jordan frame action, which is the same model

as considered in [6]. Similar models have also been considered in [7, 8]. Re-writing the model as a scalar-tensor theory of gravity plus additional scalar, and transforming to the Einstein frame, this model takes the form of a two-field inflation model with a non-flat field space. One of the fields, often referred to as the scalaron, corresponds to the additional scalar degree of freedom associated with the  $R^2$  term in the original action, and the second is simply the field we have introduced by hand. In addition to the non-flat field space, the potential in the Einstein frame also contains interactions between the two fields.

In analyzing the inflationary predictions of this model we make use of the separate Universe approach and  $\delta N$  formalism [9–14]. Due to the non-flat field space and interaction terms in the potential, it is not possible to calculate  $\delta N (= \zeta)$  analytically, and so we rely on numerical calculations. Making the slow-roll approximation, such that only the initial field positions need to be specified in solving the inflationary dynamics, the model essentially contains four parameters: the masses of the two fields and their initial positions. We explore how the inflationary dynamics and predictions for the correlation functions of  $\zeta$  depend on these four parameters, and using current observational data we put constraints on the masses of the two fields.

The paper is organised as follows. In Sec. 2, we explain the concrete set-up of our model and present the background field equations. In Sec. 3 we then review the separate Universe approach and  $\delta N$  formalism, which is used to determine the two- and three-point correlation functions of the curvature perturbation. In Sec. 4 we briefly describe our numerical method and present the results of our analysis. Our findings are then summarised in Sec. 5.

## 2 Set-up and background equations

The model we consider contains an  $R^2$  term and an additional scalar field  $\chi$  with a canonical kinetic term. We further assume that the potential for the  $\chi$  field is a simple quadratic. The action of this model is thus given by

$$S_J = \int d^4x \sqrt{-\tilde{g}} \left[ \frac{M_{pl}^2}{2} \tilde{R} + \frac{\mu}{2} \tilde{R}^2 \right] + \int d^4x \sqrt{-\tilde{g}} \left[ -\frac{1}{2} \tilde{g}^{\mu\nu} \partial_\mu \chi \partial_\nu \chi - \frac{1}{2} m_\chi^2 \chi^2 \right]. \quad (2.1)$$

Here the subscript  $J$  denotes the Jordan frame,  $\tilde{g}_{\mu\nu}$  is the Jordan frame metric,  $\tilde{R}$  is the Ricci scalar constructed from  $\tilde{g}_{\mu\nu}$  and its derivatives,  $M_{pl} = 1/\sqrt{8\pi G}$  is the reduced Planck mass, where  $G$  is Newton’s gravitational constant, and  $\mu$  is a dimensionless parameter. In analyzing the above model it is useful to re-write it as a model containing two scalar fields and a canonical Einstein-Hilbert term, which can be achieved as follows, see e.g. [15]. First we introduce the auxiliary field  $\varphi$ , and consider the action

$$S_{J\text{ Grav}} = \frac{M_{pl}^2}{2} \int d^4x \sqrt{-\tilde{g}} (f(\varphi) + f_{,\varphi}(\varphi)(R - \varphi)), \quad (2.2)$$

where  $f(\varphi) = \varphi + \mu\varphi^2/M_{pl}^2$  and  $f_{,\varphi} = df/d\varphi$ . Minimizing this action with respect to  $\varphi$  gives the constraint

$$\frac{2\mu}{M_{pl}^2} (R - \varphi) = 0, \quad (2.3)$$

which for non-zero  $\mu$  gives  $\varphi = R$ . On substituting  $\varphi = R$  into (2.2) we recover the gravitational part of (2.1), which confirms the equivalence of these two actions. Next we introduce

$e^{2\alpha\phi} = 1 + 2\mu\varphi/M_{pl}^2$  with  $\alpha = 1/(\sqrt{6}M_{pl})$ , such that (2.2) takes the form

$$S_{J\text{ Grav}} = \int d^4x \sqrt{-\tilde{g}} \left( \frac{M_{pl}^2}{2} e^{2\alpha\phi} \tilde{R} - \tilde{V}(\phi) \right), \quad \tilde{V}(\phi) = \frac{M_{pl}^4}{8\mu} (e^{2\alpha\phi} - 1)^2. \quad (2.4)$$

Thus we have re-written the gravitational part of the action given in eq. (2.1) as a scalar-tensor theory with a non-minimal coupling between the scalar field  $\phi$  and gravity. Note, however, that there is no kinetic term for the  $\phi$  field in this representation. Finally we make a conformal transformation of the metric, expressing the Jordan frame metric  $\tilde{g}_{\mu\nu}$  in terms of the so-called Einstein frame metric  $g_{\mu\nu}$  as

$$g_{\mu\nu} = \Omega^2 \tilde{g}_{\mu\nu}, \quad \text{where} \quad \Omega^2 = e^{2\alpha\phi}. \quad (2.5)$$

On doing so we find that the total action takes the form

$$S_E = \int d^4x \sqrt{-g} \left[ \frac{M_{pl}^2}{2} R - \frac{g^{\mu\nu}}{2} (\partial_\mu \phi) (\partial_\nu \phi) - \frac{1}{2} g^{\mu\nu} e^{-2\alpha\phi} (\partial_\mu \chi) (\partial_\nu \chi) - V(\phi, \chi) \right], \quad (2.6)$$

with

$$V(\phi, \chi) = \frac{3}{4} m_\phi^2 M_{pl}^2 (1 - e^{-2\alpha\phi})^2 + \frac{1}{2} m_\chi^2 e^{-4\alpha\phi} \chi^2. \quad (2.7)$$

Here we introduced  $m_\phi^2 = M_{pl}^2/(6\mu)$  and the subscript  $E$  denotes the Einstein frame. The label ‘Einstein frame’ is appropriate given that the gravity part of the action now takes the canonical Einstein-Hilbert form, which is somewhat easier to analyze than the gravity sector of the original action (2.1). Note, however, that reducing the gravity sector to the canonical Einstein-Hilbert form has come at the cost of introducing the additional scalar degree of freedom  $\phi$  — often referred to as the scalaron — and interaction terms between the two fields  $\phi$  and  $\chi$ , which appear in the second term of the potential and in the kinetic term of  $\chi$ .

Using a more abstract notation, the action (2.6) can be re-written in the form of a non-linear sigma model as

$$S_E = \int d^4x \sqrt{-g} \left[ \frac{M_{pl}^2}{2} R - \frac{1}{2} \mathcal{G}_{IJ} g^{\mu\nu} \partial_\mu \phi^I \partial_\nu \phi^J - V(\phi^I) \right]. \quad (2.8)$$

In our case the Latin indices  $I$  and  $J$  take on the values  $\phi$  and  $\chi$ , with  $\phi^\phi = \phi$  and  $\phi^\chi = \chi$ .  $\mathcal{G}_{IJ}$  is interpreted as the metric on field space, and in our case the components are given as

$$\mathcal{G}_{\phi\phi} = 1, \quad \mathcal{G}_{\chi\chi} = e^{-2\alpha\phi}, \quad \mathcal{G}_{\phi\chi} = \mathcal{G}_{\chi\phi} = 0. \quad (2.9)$$

Varying the action (2.8) with respect to  $g_{\mu\nu}$ , assuming a Friedmann-Lemaitre-Robertson-Walker (FLRW) metric of the form  $g_{\mu\nu} = \text{diag}(-1, a^2(t), a^2(t), a^2(t))$  and taking the scalar fields to be homogeneous, namely  $\phi^I = \phi^I(t)$ , we obtain the Friedmann equation

$$H^2 = \frac{1}{3M_{pl}^2} \left[ \frac{1}{2} \mathcal{G}_{IJ} \dot{\phi}^I \dot{\phi}^J + V(\phi^I) \right], \quad (2.10)$$

and the continuity equation

$$\dot{H} = -\frac{1}{2M_{pl}^2} \mathcal{G}_{IJ} \dot{\phi}^I \dot{\phi}^J, \quad (2.11)$$

where  $H = \dot{a}/a$  and an overdot denotes taking the derivative with respect to time. The equations of motion for the homogeneous fields  $\phi^I$  are given as

$$\mathcal{D}_t \dot{\phi}^I + 3H\dot{\phi}^I + \mathcal{G}^{IJ}V_{,J} = 0, \quad (2.12)$$

where  $V_{,J} = \partial V/\partial \phi^J$  and we have introduced the covariant time derivative  $\mathcal{D}_t$  that acts as  $\mathcal{D}_t X^I = \dot{X}^I + \Gamma^I_{JK} \dot{\phi}^J X^K$ , with the Christoffel symbols  $\Gamma^I_{JK}$  being constructed from  $\mathcal{G}_{IJ}$  and its derivatives (see Appendix for details). In our case, the equations of motion for  $\phi$  and  $\chi$  are given as

$$\ddot{\phi} + 3H\dot{\phi} + \alpha e^{-2\alpha\phi} \dot{\chi}^2 + V_{,\phi} = 0, \quad (2.13)$$

$$\ddot{\chi} + 3H\dot{\chi} - 2\alpha\dot{\phi}\dot{\chi} + e^{2\alpha\phi} V_{,\chi} = 0. \quad (2.14)$$

In the context of inflation, it is useful to define the slow-roll parameters  $\epsilon = -\dot{H}/H^2$  and  $\eta = \dot{\epsilon}/(\epsilon H)$ . In order to obtain quasi-exponential inflation we require  $\epsilon \ll 1$ , and the condition  $\eta \ll 1$  ensures that inflation lasts for long enough.<sup>1</sup> The amount of inflation is parameterised in terms of the  $e$ -folding number  $N$  defined as

$$N(t, t_*) = \int_{t_*}^t H(t) dt = \ln \left( \frac{a(t)}{a(t_*)} \right), \quad (2.15)$$

where  $t_*$  is the initial time, and observational constraints dictate that  $N \gtrsim 60$ . In terms of the scalar fields, we have

$$\epsilon = \frac{1}{2M_{pl}^2} \frac{\mathcal{G}_{IJ} \dot{\phi}^I \dot{\phi}^J}{H^2} \quad \text{and} \quad \eta = 2\epsilon + 2 \frac{\mathcal{G}_{IJ} \dot{\phi}^I \mathcal{D}_t \dot{\phi}^J}{H \mathcal{G}_{KL} \dot{\phi}^K \dot{\phi}^L}. \quad (2.16)$$

The slow-roll condition  $\epsilon \ll 1$  thus implies that

$$H^2 \simeq \frac{V(\phi^I)}{3M_{pl}^2}. \quad (2.17)$$

Given that  $\epsilon \ll 1$ , the condition  $\eta \ll 1$  implies that

$$\frac{\mathcal{G}_{IJ} \dot{\phi}^I \mathcal{D}_t \dot{\phi}^J}{H \mathcal{G}_{KL} \dot{\phi}^K \dot{\phi}^L} \ll 1. \quad (2.18)$$

In the single-field case, where we can always redefine the field such that  $\mathcal{G}_{\phi\phi} = 1$ , this reduces to  $\ddot{\phi} \ll H\dot{\phi}$ , which allows us to neglect the acceleration term in the equation of motion for  $\phi$ . In the multi-field case with a curved field space, however, the situation is not so simple, as the above condition only constrains the component of  $\mathcal{D}_t \dot{\phi}^I$  along the background trajectory. Nevertheless, we assume that the magnitude of the acceleration vector  $\mathcal{D}_t \dot{\phi}^I$  is much smaller than the magnitude of the velocity vector  $H\dot{\phi}^I$ , namely  $(\mathcal{G}_{IJ} \mathcal{D}_t \dot{\phi}^I \mathcal{D}_t \dot{\phi}^J)^{1/2} \ll H(\mathcal{G}_{IJ} \dot{\phi}^I \dot{\phi}^J)^{1/2}$ . By the Cauchy-Schwarz inequality, this will guarantee that condition (2.18) is satisfied. If we further assume that the field basis is such that  $|\mathcal{D}_t \dot{\phi}^I| \ll |H\dot{\phi}^I|$  for all  $I$ , where here by  $|X^I|$  we mean the magnitude of the  $I$ th component of  $X^I$ , then the equations of motion (2.12) reduce to

$$3H\dot{\phi}^I \simeq -\mathcal{G}^{IJ}V_{,J}, \quad (2.19)$$

---

<sup>1</sup>Strictly speaking  $\eta$  can be negative. So we take slow-roll to mean that  $|\eta| \ll 1$ .

meaning that we are in an attractor regime where the field velocities are given as functions of the field positions. Using the slow-roll equations (2.17) and (2.19) we can then derive consistency conditions for the potential and its derivatives. Namely, we find

$$\epsilon \simeq \epsilon_V = \frac{M_{pl}^2}{2} \frac{\mathcal{G}^{IJ} V_{,I} V_{,J}}{V^2} \ll 1, \quad \eta \simeq \eta_V = 4\epsilon_V - \frac{M_{pl}^4}{\epsilon_V} \frac{\mathcal{D}_K V_{,J} \mathcal{G}^{KL} V_{,L} \mathcal{G}^{JM} V_{,M}}{V^3} \ll 1, \quad (2.20)$$

where  $\mathcal{D}_K V_{,J} = V_{,JK} - \Gamma_{JK}^L V_{,L}$  is the covariant derivative of  $V_{,J}$ . The first condition  $\epsilon_V \ll 1$  thus puts a constraint on the first derivatives of  $V$ , while the condition  $\eta_V \ll 1$  constrains the second derivatives of  $V$ . In particular, assuming  $\epsilon_V \ll 1$ , the condition  $\eta_V \ll 1$  will be satisfied if we assume that all the eigenvalues of the field-space tensor  $\eta_J^I$  are small, where  $\eta_J^I$  is defined as

$$\eta_J^I \equiv M_{pl}^2 \frac{\mathcal{G}^{IK} \mathcal{D}_J V_{,K}}{V}. \quad (2.21)$$

Provided the number of fields is not too large, the Eigenvalues of  $\eta_J^I$  will in turn be small if  $\eta_J^I \ll 1$  for all  $I$  and  $J$ . Note that the quantity  $\eta_J^I$  corresponds to the covariant Hessian of the potential divided by  $V/M_{pl}^2 \simeq 3H^2$ , and the covariant Hessian of the potential contributes to the effective mass matrix of field fluctuations about the background trajectory, see e.g. [9]. As such, the condition  $\eta_J^I \ll 1$  will constitute part of the sufficient condition for the effective mass of field fluctuations to be small compared to the Hubble scale.

### 3 $\zeta$ and its correlation functions using the $\delta N$ formalism

Having introduced the model and background equations in the previous section, we now move on to consider perturbations. In particular, we are interested in determining the so-called curvature perturbation on constant density slices,  $\zeta$ , as it is this quantity that can be related to the temperature fluctuations observed in the CMB. More precisely, we are interested in the correlation functions of  $\zeta$ , as it is only the statistical properties of the CMB temperature fluctuations that we are able to make predictions for.

In general, following the notation of [14], the full perturbed metric can be written in the form

$$ds^2 = -\alpha^2 dt^2 + a^2(t) e^{2\psi} \gamma_{ij} (dx^i + \beta^i dt) (dx^j + \beta^j dt), \quad (3.1)$$

where  $\gamma_{ij}$  has unit determinant and can be written in terms of the traceless tensor  $h_{ij}$  as  $\gamma_{ij} = (e^h)_{ij}$ .  $h_{ij}$  can itself be decomposed as

$$h_{ij} = \partial_i C_j + \partial_j C_i - \frac{2}{3} \delta_{ij} \partial_k C_k + h_{ij}^{(T)}, \quad (3.2)$$

where  $C_i$  contains both scalar and vector perturbations and  $h_{ij}^{(T)}$ , satisfying  $\partial_i h_{ij}^{(T)} = 0$ , corresponds to tensor perturbations. In addition to metric perturbations, we also have the perturbed scalar fields  $\hat{\phi}^I(t, \mathbf{x}) = \phi^I(t) + \delta\phi^I(t, \mathbf{x})$ . The density associated with their energy-momentum tensor is similarly decomposed as  $\hat{\rho}(t, \mathbf{x}) = \rho(t) + \delta\rho(t, \mathbf{x})$ . Following [14], we make use of the flat threading, in which  $C_i = 0$ , and the curvature perturbation on constant density slices,  $\zeta$ , then corresponds to  $\psi$  evaluated in the gauge where  $\delta\rho = C_i = 0$ , namely  $\zeta = \psi|_{\delta\rho=C_i=0}$ .

## Separate Universe approach and the $\delta N$ expansion

In order to determine  $\zeta$  and its correlation functions we make use of the separate Universe approach and the  $\delta N$  formalism [9–14]. The separate Universe approach corresponds to the leading order approximation in a gradient expansion. One first assumes that the characteristic length scale of spatial variations,  $L$ , is longer than the Hubble scale, namely  $\xi = 1/(HL) \ll 1$ . Associating a factor of  $\xi$  with spatial gradients appearing in the field equations, one can then perform an expansion in the parameter  $\xi$ . Neglecting terms of order  $\xi^2$  and higher, one finds that the field equations take on exactly the same form as the background equations. In other words, separate super-Hubble sized patches are found to evolve as separate background Universes, differing only in their initial conditions. If we are interested in a comoving scale with wavenumber  $k$ , during inflation the parameter  $\xi = k/(aH)$  will be decreasing exponentially with time. As such, the separate Universe approach will become applicable after the Horizon-crossing time, which is defined as the time at which  $k = aH$ .

Making use of the flat gauge, corresponding to  $\psi = C_i = 0$ , the validity of the separate Universe approach in the case of multiple scalar fields has been confirmed explicitly to all orders in perturbation theory by Sugiyama *et al.* [14].  $\beta^i$  and  $\dot{h}_{ij}^{(T)}$  were shown to decay away on super-horizon scales, such that the field equations indeed take on exactly the same form as the background equations, namely

$$\hat{H}^2 = \frac{1}{3M_{pl}^2} \left[ \frac{1}{2} \partial_\tau \hat{\phi}^I \partial_\tau \hat{\phi}^J + V(\hat{\phi}^I) \right], \quad (3.3)$$

$$\mathcal{D}_\tau \partial_\tau \hat{\phi}^I + 3\hat{H} \partial_\tau \hat{\phi}^I + \mathcal{G}^{IJ} V_{,J}(\hat{\phi}^K) = 0 \quad (3.4)$$

where  $\hat{H}(t, \mathbf{x}) = H(t)/\alpha(t, \mathbf{x})$  is the local Hubble expansion and  $\partial_\tau = \partial/\partial\tau$ , with  $d\tau = \alpha(t, \mathbf{x})dt$ . A result that proves very useful is that the local  $e$ -folding number is found to be unperturbed [9, 12], as

$$\hat{N} = \int \hat{H} d\tau = \int H dt. \quad (3.5)$$

This can also be understood if, associated with the perturbed metric in eq. (3.1), we define the effective scale factor  $\hat{a}(t, \mathbf{x}) = a(t)e^{\psi(t, \mathbf{x})}$ . The local  $e$ -folding number is then given as

$$\hat{N} = \ln \left( \frac{\hat{a}}{\hat{a}_*} \right) = \psi - \psi_* + N, \quad (3.6)$$

and in the flat slicing, i.e.  $\psi = \psi_* = 0$ , this reduces to the background  $e$ -folding number. The  $e$ -folding number is thus a useful time parameter in the flat gauge, and given that the field equations (3.3) and (3.4) take on the same form as the background equations, we are able to write

$$\hat{\phi}^I(N, \mathbf{x}) = \phi^I(N, \phi_*^J(\mathbf{x})), \quad (3.7)$$

where  $\phi^I(N, \phi_*^J(\mathbf{x}))$  is a solution of the background equations of motion with the spatially dependent initial conditions  $\phi^I(t_*) = \phi_*^I(\mathbf{x})$ .<sup>2</sup> In other words, the value of  $\hat{\phi}^I$  at a given location  $\mathbf{x}$  is found simply by solving the background equations of motion with the appropriate initial conditions for that location.

<sup>2</sup>In principle we also need to specify the initial field velocities, but we will assume that the slow-roll approximation is valid around the time of horizon crossing, such that field velocities are given in terms of the field values as in eq. (2.19).

Having outlined the separate Universe approach, we now wish to determine  $\zeta$ , and for this we use the  $\delta N$  formalism [9, 10, 12, 14]. The basic idea of the  $\delta N$  formalism is that  $\zeta$  on some final uniform density slice can be given in terms of the spatial fluctuations of the  $e$ -folding number between an initial spatially flat slice and the final uniform density slice. This can be understood if we look at the expression for the local  $e$ -folding number given in (3.6). Taking the initial slice to be flat and the final slice to be a constant density one, corresponding to  $\psi_* = 0$  and  $\psi = \zeta$ , we find  $\delta N = \hat{N} - N = \zeta$ . Note that it does not matter exactly when we take the initial flat slice, as it is only important that  $\psi_* = 0$ . The only restriction is that  $t_*$  must be after the time at which the scales under consideration have left the horizon.

The next step in the  $\delta N$  formalism is to show that  $\delta N$  can be expanded in terms of the field perturbations on the initial flat slice,  $\delta\phi_*^I(\mathbf{x})$ . To see this, recall that in the context of the separate Universe approach the field equations take on exactly the same form as the background equations. As mentioned above, this means that the solutions for  $\hat{\phi}^I(N, \mathbf{x})$  in the flat gauge are as given in eq. (3.7), i.e. they are solutions to the background equations but with the initial conditions varying from place to place. Similarly, it also means that the energy density on flat slices can be expressed as

$$\hat{\rho}(N, \mathbf{x}) = \rho(N, \phi_*^I(\mathbf{x})), \quad (3.8)$$

where  $\rho(N, \phi_*^I(\mathbf{x}))$  is the density as determined by solving the background field equations with the spatially inhomogeneous initial conditions  $\phi^I(t_*) = \phi_*^I(\mathbf{x})$ . In general  $\hat{\rho}(N, \mathbf{x})$  is not spatially homogeneous, and if we assume that the initial conditions at position  $\mathbf{x}$  can be expanded about the initial conditions of the fiducial background trajectory as  $\phi_*^I(\mathbf{x}) = \phi_*^I + \delta\phi_*^I(\mathbf{x})$ , this leads to an expansion of the form

$$\hat{\rho}(N, \mathbf{x}) = \rho(N, \phi_*^I) + \rho_{,I}(N, \phi_*^J)\delta\phi_*^I(\mathbf{x}) + \frac{1}{2}\rho_{,IJ}(N, \phi_*^K)\delta\phi_*^I(\mathbf{x})\delta\phi_*^J(\mathbf{x}) + \dots, \quad (3.9)$$

where  $\rho(N, \phi_*^I)$  is the density of the fiducial background trajectory,  $\rho_{,I}(N, \phi_*^J) = \partial\rho(N, \phi_*^J)/\partial\phi_*^I$  and similarly for  $\rho_{,IJ}(N, \phi_*^K)$ . At each location  $\mathbf{x}$ , we can then consider the shift along the local trajectory,  $\delta N$ , that is required to reach a constant density slice. In other words, at each location  $\mathbf{x}$  we find the shift in  $N$  such that  $\hat{\rho}(N + \delta N, \mathbf{x}) = \rho(N, \phi_*^I)$ . Given the form of the expansion for  $\hat{\rho}(N, \mathbf{x})$  in eq. (3.9), solving  $\hat{\rho}(N + \delta N, \mathbf{x}) = \rho(N, \phi_*^I)$  gives rise to an expansion of the form

$$\zeta(N, \mathbf{x}) = \delta N(N, \mathbf{x}) = N_{,I}(N, \phi_*^J)\delta\phi_*^I(\mathbf{x}) + \frac{1}{2}N_{,IJ}(\phi_*^K)\delta\phi_*^I(\mathbf{x})\delta\phi_*^J(\mathbf{x}) + \dots, \quad (3.10)$$

which is the famous  $\delta N$  expansion. As mentioned above, in principle the initial flat slice can be taken to be at any time after the scales under consideration have left the horizon, but in practice it is useful to choose it to coincide with the horizon crossing time, as expressions for the quantities  $\delta\phi_*^I(\mathbf{x})$  and their correlations at this time are known [9, 16].

While the above form for the expansion of  $\zeta$  is perfectly acceptable, in the case of a curved field space the field perturbations  $\delta\phi_*^I(\mathbf{x}) = \phi_*^I(\mathbf{x}) - \phi_*^I$ , which correspond to coordinate displacements, do not transform covariantly. In order to obtain an explicitly covariant expression for  $\zeta$  we follow the discussion in [17], see also [18, 19]. For sufficiently small  $\delta\phi_*^I(\mathbf{x})$ , the two points in field space  $\phi_*^I(\mathbf{x})$  and  $\phi_*^I$  are connected by a unique geodesic that we take to be parameterised by  $\lambda$ . Normalising  $\lambda$  such that  $\phi^I(\lambda = 0) = \phi_*^I$ , and  $\phi^I(\lambda = 1) = \phi_*^I(\mathbf{x})$ ,



we can obtain a Taylor series expansion for  $\delta\phi^I = \phi^I(\lambda = 1) - \phi^I(\lambda = 0)$  as

$$\delta\phi^I = \left. \frac{d\phi^I}{d\lambda} \right|_{\lambda=0} + \frac{1}{2} \left. \frac{d^2\phi^I}{d\lambda^2} \right|_{\lambda=0} + \dots \quad (3.11)$$

On the other hand, the geodesic satisfies

$$\mathcal{D}_\lambda \frac{d\phi^I}{d\lambda} \equiv \frac{d^2\phi^I}{d\lambda^2} + \Gamma^I_{JK} \frac{d\phi^J}{d\lambda} \frac{d\phi^K}{d\lambda} = 0. \quad (3.12)$$

As such, introducing  $\mathcal{Q}^I = d\phi^I/d\lambda|_{\lambda=0}$ , which resides in the tangent space at  $\phi^I(\lambda = 0)$  and thus transforms covariantly, we can express  $\delta\phi^I$  in terms of  $\mathcal{Q}^I$  as

$$\delta\phi^I = \mathcal{Q}^I - \frac{1}{2!} \Gamma^I_{JK} \mathcal{Q}^J \mathcal{Q}^K + \dots \quad (3.13)$$

Inserting this relation into (3.10) we obtain

$$\zeta(N, \mathbf{x}) = N_{,I} N(N, \phi_*^J) \mathcal{Q}_*^I(\mathbf{x}) + \frac{1}{2} \mathcal{D}_I \mathcal{D}_J N(N, \phi_*^K) \mathcal{Q}_*^I(\mathbf{x}) \mathcal{Q}_*^J(\mathbf{x}) + \dots, \quad (3.14)$$

which is now explicitly covariant.

### The power spectrum and bispectrum of $\zeta$

Having obtained an expansion for  $\zeta$  in terms of the covariantised field perturbations on a flat slice at the horizon crossing time, we now turn to the correlation functions of  $\zeta$ . Working in Fourier space, the two-point correlation function of  $\zeta$  is parameterised as

$$\langle \zeta(\mathbf{k}_1) \zeta(\mathbf{k}_2) \rangle = (2\pi)^3 \delta^3(\mathbf{k}_1 + \mathbf{k}_2) P_\zeta(k_1) = (2\pi)^3 \delta(\mathbf{k}_1 + \mathbf{k}_2) \frac{2\pi^2}{k_1^3} \mathcal{P}_\zeta(k_1), \quad (3.15)$$

and the three-point correlation function is similarly parameterised as

$$\langle \zeta(\mathbf{k}_1) \zeta(\mathbf{k}_2) \zeta(\mathbf{k}_3) \rangle = (2\pi)^3 \delta^3(\mathbf{k}_1 + \mathbf{k}_2 + \mathbf{k}_3) B_\zeta(k_1, k_2, k_3). \quad (3.16)$$

$P_\zeta(k)$  and  $\mathcal{P}_\zeta(k)$  are the power spectrum and reduced power spectrum, respectively, while  $B_\zeta(k_1, k_2, k_3)$  is the bispectrum. In both (3.15) and (3.16) the delta functions are a consequence of assuming statistical homogeneity, and the fact that  $P_\zeta$ ,  $\mathcal{P}_\zeta$  and  $B_\zeta$  depend only on the magnitudes of  $\mathbf{k}_i$  is a consequence of assuming statistical isotropy. In relation to the three-point function, a useful parameter introduced to quantify the level of non-Gaussianity is  $f_{NL}$ , which is defined as

$$f_{NL} = \frac{5}{6} \frac{B_\zeta(k_1, k_2, k_3)}{P_\zeta(k_1) P_\zeta(k_2) + \text{c.p.}}, \quad (3.17)$$

where c.p. denotes cyclic permutations of  $k_1$ ,  $k_2$  and  $k_3$ . Given the expansion for  $\zeta$  in eq. (3.14), we see that the correlation functions of  $\zeta$  can be expressed in terms of the correlation functions of the covariantised field perturbations on the initial flat slice,  $\mathcal{Q}^I$ . In particular, we have

$$\langle \zeta(\mathbf{k}_1) \zeta(\mathbf{k}_2) \rangle = N_{,I} N_{,J} \langle \mathcal{Q}_*^I(\mathbf{k}_1) \mathcal{Q}_*^J(\mathbf{k}_2) \rangle, \quad (3.18)$$

$$\langle \zeta(\mathbf{k}_1) \zeta(\mathbf{k}_2) \zeta(\mathbf{k}_3) \rangle = N_{,I} N_{,J} N_{,K} \langle \mathcal{Q}_*^I(\mathbf{k}_1) \mathcal{Q}_*^J(\mathbf{k}_2) \mathcal{Q}_*^K(\mathbf{k}_3) \rangle \quad (3.19)$$

$$+ N_{,I} N_{,J} \mathcal{D}_K \mathcal{D}_L N \int \frac{d^3\mathbf{q}}{(2\pi)^3} \langle \mathcal{Q}_*^K(\mathbf{k}_1 - \mathbf{q}) \mathcal{Q}_*^I(\mathbf{k}_2) \rangle \langle \mathcal{Q}_*^L(\mathbf{q}) \mathcal{Q}_*^J(\mathbf{k}_3) \rangle + \text{c.p.},$$

where for brevity we drop the arguments of  $N_{,I}$  and  $\mathcal{D}_J \mathcal{D}_I N$ . The contribution to the three-point correlation function of  $\zeta$  coming from the first term involving the three-point correlation functions of  $\mathcal{Q}^I$  is known to be unobservably small [20, 21], so in proceeding we choose to neglect it. As such, the only quantities required are the two-point correlation functions of  $\mathcal{Q}^I$ . At linear order in perturbations we have  $\mathcal{Q}^I = \delta\phi^I$ , and the two-point correlation functions of  $\delta\phi^I$  in the case of a curved field space have been calculated in [9, 16]. The result at lowest order in slow-roll is

$$\langle \mathcal{Q}_*^I(\mathbf{k}_1) \mathcal{Q}_*^J(\mathbf{k}_2) \rangle = (2\pi)^3 \delta^3(\mathbf{k}_1 + \mathbf{k}_2) \frac{2\pi^2}{k_1^3} \left( \frac{H_*}{2\pi} \right)^2 \mathcal{G}_*^{IJ}, \quad (3.20)$$

where recall that an asterisk now denotes that a quantity should be evaluated at the time of horizon crossing, namely  $k_1 = a_* H_*$ . Substituting this result into eqs. (3.18) and (3.19), expressions for  $\mathcal{P}_\zeta(k_1)$  and  $f_{NL}$  are obtained as

$$\mathcal{P}_\zeta(k) = \left( \frac{H_*}{2\pi} \right)^2 \mathcal{G}_*^{IJ} N_{,I} N_{,J}, \quad (3.21)$$

$$f_{NL} = \frac{5}{6} \frac{N_{,I} N_{,J} \mathcal{D}_I \mathcal{D}_J N}{(N_{,K} N_{,K})^2}, \quad (3.22)$$

where the raised indices in the second expression are raised with  $\mathcal{G}_*^{IJ}$ .

In addition to the above two observables, we also consider the tilt of the power spectrum,  $n_s$ , and the tensor-to-scalar ratio,  $r$ . The tilt of the power spectrum is defined through the relation

$$\mathcal{P}_\zeta(k) = A_s \left( \frac{k}{k_p} \right)^{n_s - 1}, \quad (3.23)$$

where  $k_p$  is some pivot scale and  $A_s$  gives the magnitude of  $\mathcal{P}_\zeta$  at the pivot scale. The scale dependence of  $\mathcal{P}_\zeta$  as given in eq. (3.21) appears through its dependence on quantities evaluated at the horizon crossing time of the comoving scale  $k$ . We do not present a detailed derivation here, but the final result is given as [9]

$$n_s = 1 - 2\epsilon_* - 2 \frac{1 + N_{,I} \left( \frac{1}{3} R^{IJKL} \frac{V_{,J} V_{,K}}{V^2} - \frac{\mathcal{D}^I \mathcal{D}^L V}{V} \right)_* N_{,L}}{N_{,M} N_{,M}}, \quad (3.24)$$

where,  $R^{IJKL}$  is the curvature tensor constructed from  $\mathcal{G}_{IJ}$ . Note that  $A_s$  is found simply by taking  $k = k_p$  in eq. (3.21).

Finally, the tensor-to-scalar ratio is defined as the ratio between the power spectra of tensor and scalar perturbations. In particular, if we parameterise the power spectrum of tensor perturbations as

$$\mathcal{P}_T(k) = A_T \left( \frac{k}{k_p} \right)^{n_T}, \quad (3.25)$$

then we have  $r = A_T/A_s$ . It can be shown that  $A_T = 8(H_*/(2\pi))^2/M_{pl}^2$ , see e.g. [22], such that we obtain

$$r = \frac{8}{M_{pl}^2 N_{,I} N_{,I}}. \quad (3.26)$$

## Observational bounds

In general, as indicated in eq. (3.14),  $\zeta$  will depend on time. As such, when trying to compare the predictions of a particular model with observational constraints it is important that we choose an appropriate time at which to evaluate  $\zeta$ . In the case of single-field inflation it is known that even for a very general class of models  $\zeta$  is conserved on super-horizon scales, see e.g. [23, 24], which means that the appropriate time to evaluate  $\zeta$  is shortly after the scales under consideration left the horizon. In the multi-field case, however,  $\zeta$  can continue to evolve on super-horizon scales, and so it becomes necessary to follow the evolution of  $\zeta$  up until a so-called adiabatic limit is reached and  $\zeta$  becomes conserved.<sup>3</sup> The non-conservation of  $\zeta$  during inflation results from it being sourced by so-called isocurvature perturbations when the background trajectory deviates from a geodesic of the field space, see e.g. [25, 26]. Isocurvature perturbations are field perturbations orthogonal to the background trajectory, and an adiabatic limit corresponds to the situation where all isocurvature perturbations have decayed away, leaving only perturbations along the trajectory. With no isocurvature modes to source  $\zeta$  it becomes conserved, and the fact that only perturbations along the trajectory — adiabatic perturbations — remain means that an adiabatic limit corresponds to an effectively single-field limit. If isocurvature modes have not decayed away by the end of inflation, then one must continue to following the evolution of  $\zeta$  through (p)reheating. An analysis of (p)reheating in the model under consideration, however, is beyond the scope of this paper, and will very much depend on how the fields  $\phi$  and  $\chi$  in eq. (2.6) are coupled to other forms of matter.<sup>4</sup> As such, in the following we will focus on the evolution of  $\zeta$  during inflation and its properties at the end of inflation. In cases where an adiabatic limit is reached before the end of inflation we are justified in comparing our results with observational constraints, and we will point out when this is not the case and evolution of  $\zeta$  through (p)reheating may be important.

Closely related to the issue of whether or not an adiabatic limit is reached is the issue of frame-dependence. Most of our discussion up to now has been centred on the Einstein-frame representation of the model given in eq. (2.6), but we could equally have chosen to perform our analysis in the original Jordan-frame representation. At the classical level the two representations simply correspond to a re-labelling of the metric, and if we perform calculations consistently then predictions for observable quantities should be independent of the choice of frame. The physical picture in the two frames, however, may be very different, see e.g. [28]. Indeed, in the context of inflation, at the level of the background the definition of inflation is not even a frame-independent notion, and it is possible to have a situation where the FLRW metric in one frame is inflating while that in the other is not, see e.g. [29]. At the level of perturbations, however, the situation is fortunately somewhat simpler. Tensor perturbations are left unchanged by a conformal transformation, and  $\zeta$  is also frame-independent in the single-field case or in the case that an adiabatic limit has been reached [30–32]. Only in the case that isocurvature perturbations remain does one have to be a little more careful, as  $\zeta$  is not necessarily frame-independent in this case [33–35]. Note that this does not imply an inequivalence between the two frames, but simply indicates that the quantity  $\zeta$  itself does not yet directly correspond to an observable quantity. As discussed above, independent of the frame issue it becomes necessary to follow the evolution of  $\zeta$  through (p)reheating in the case that an adiabatic limit is not reached by the end of inflation, and we will not address

---

<sup>3</sup>It is also possible that a so-called adiabatic limit is not reached, but non-adiabatic contributions to the CMB temperature fluctuations are now tightly constrained [1].

<sup>4</sup>One choice of matter and coupling is considered in [27].

this issue here. In this sense, the potential frame-dependence of  $\zeta$  will only affect the cases for which we are already not justified in comparing our results with observations, so we postpone addressing the issue in any more detail. Note that for our particular model the Jordan and Einstein frames will coincide once the field  $\phi$  relaxes to  $\phi = 0$ .

With the above remarks in mind, the observational constraints on  $A_s$ ,  $n_s$ ,  $r$  and  $f_{NL}$  with which we compare our results are those presented by the *Planck* collaboration [1]. Taking a pivot scale of  $k_p = 0.05 \text{ Mpc}^{-1}$  they find

$$A_s = (2.21 \pm 0.07) \times 10^{-9} \quad (68\% \text{ C.L.}), \quad (3.27)$$

$$n_s = 0.968 \pm 0.006 \quad (68\% \text{ C.L.}), \quad (3.28)$$

$$r < 0.11 \quad (95\% \text{ C.L.}), \quad (3.29)$$

$$f_{NL} = 0.8 \pm 5.0 \quad (68\% \text{ C.L.}). \quad (3.30)$$

## 4 Numerical analysis and results

As can be seen from the expressions given in eqs. (3.21), (3.22), (3.24) and (3.26), the observables  $\mathcal{P}_\zeta$ ,  $n_s$ ,  $r$  and  $f_{NL}$  for a given inflationary trajectory can be determined with knowledge of the background dynamics alone, which is one of the very appealing aspects of the  $\delta N$  formalism. In particular, we require the background quantities  $H$ ,  $\epsilon$ ,  $\mathcal{G}_{IJ}$  and  $V$  evaluated at the horizon-crossing time of the comoving scale under consideration, as well as the derivatives of the  $e$ -folding number up to a constant density surface with respect to the field values at the horizon crossing time,  $N_{,I}$  and  $\mathcal{D}_J \mathcal{D}_I N$ . For a restricted class of potentials and field-space metrics it is possible to determine the derivatives of  $N$  analytically if the slow-roll equations of motion (2.19) are assumed to hold throughout inflation, see e.g. [36–40], but in general one has to resort to numerical calculations. The model we are considering contains both a non-trivial field-space metric and interaction terms in the potential, meaning that the derivatives of  $N$  cannot be determined analytically. We thus have to take a numerical approach, the method of which we now briefly explain.

Our code is based on the finite difference method. We first consider a background trajectory with the initial conditions  $(\phi_*, \chi_*)$ , and assume that the scale under consideration left the horizon as the trajectory passed through this point. Evolving along the trajectory, at any later time of interest  $t$ , we can determine the number of  $e$ -foldings since the horizon-crossing time,  $N(t, \phi_*, \chi_*)$ , and the density at that time,  $\rho(t, \phi_*, \chi_*)$ . Next we consider another trajectory with displaced initial conditions, e.g.  $(\phi_* + \Delta\phi, \chi_*)$ . Evolving along this trajectory we determine the time  $\tilde{t} = t + \delta t$  at which the density of the displaced trajectory coincides with  $\rho(t, \phi_*, \chi_*)$ , namely  $\rho(\tilde{t}, \phi_* + \Delta\phi, \chi_*) = \rho(t, \phi_*, \chi_*)$ . We then determine the number of  $e$ -foldings that have elapsed on the perturbed trajectory from the initial time up to the time  $\tilde{t}$ ,  $N(\tilde{t}, \phi_* + \Delta\phi, \chi_*)$ . This is the number of  $e$ -foldings up to the constant density surface, and the derivative of  $N$  with respect to  $\phi_*$  is then given as

$$N_{,\phi_*} = \frac{N(\tilde{t}, \phi_* + \Delta\phi, \chi_*) - N(t, \phi_*, \chi_*)}{\Delta\phi}. \quad (4.1)$$

The same procedure applies for determining  $N_{,\chi_*}$ , and can be extended to calculate the second-order derivatives  $N_{,\phi_*\phi_*}$ ,  $N_{,\chi_*\chi_*}$  and  $N_{,\phi_*\chi_*} = N_{,\chi_*\phi_*}$ . In all our calculations we assume that the slow-roll field equations (2.17) and (2.19) are a good approximation at the time of horizon crossing. The initial field velocities are thus determined through eq. (2.19) and do not need to be specified independently. Nevertheless, we do solve the full equations

of motion eq. (2.12) when calculating the derivative of  $N$ . This allows for the possibility that the slow-roll approximation breaks down later on during the super-horizon evolution. We have worked with 32-digit precision.

Note that the time  $t$  in the above discussion can be any time after the horizon crossing time, so by varying  $t$  we can determine the evolution of  $\zeta$ . If we are interested in determining  $\zeta$  at the end of inflation, then we take  $t$  to be the time at which  $\epsilon \simeq 1$ . As discussed at the end of the previous section, if an adiabatic limit has not been reached by the end of inflation then it is necessary to follow the evolution of  $\zeta$  through (p)reheating and until an adiabatic limit is reached and  $\zeta$  becomes conserved. However, the evolution of  $\zeta$  through (p)reheating is beyond the scope of this paper, and we restrict our attention to the evolution of  $\zeta$  up until the end of inflation.

In proceeding, rather than working with the parameters  $m_\phi$  and  $m_\chi$ , we instead introduce the mass ratio defined as

$$R_{\text{mass}} \equiv \frac{m_\chi}{m_\phi}. \quad (4.2)$$

This allows an overall  $m_\phi^2$  to be factored out of the potential, namely

$$V(\phi, \chi) = m_\phi^2 \mathcal{V}(\phi, \chi), \quad \mathcal{V}(\phi, \chi) = \frac{3}{4} M_{\text{pl}}^2 (1 - e^{-2\alpha\phi})^2 + \frac{1}{2} R_{\text{mass}}^2 e^{-4\alpha\phi} \chi^2. \quad (4.3)$$

If we then introduce the re-scaled time parameter  $\tilde{\tau} = m_\phi t$ , we find that the background field equations reduce to

$$\mathcal{D}_{\tilde{\tau}} \phi_{\tilde{\tau}}^I + 3\mathcal{H} \phi_{\tilde{\tau}}^I + \mathcal{G}^{IJ} \mathcal{V}_{,J} = 0, \quad (4.4)$$

$$\mathcal{H}^2 = \frac{1}{3M_{\text{pl}}^2} \left[ \frac{1}{2} \mathcal{G}_{IJ} \phi_{\tilde{\tau}}^I \phi_{\tilde{\tau}}^J + \mathcal{V}(\phi^I) \right], \quad (4.5)$$

where a subscript  $\tilde{\tau}$  denotes taking the derivative with respect to  $\tilde{\tau}$ , e.g.  $\phi_{\tilde{\tau}}^I = d\phi^I/d\tilde{\tau}$ ,  $\mathcal{H} = a_{\tilde{\tau}}/a$  and  $\mathcal{D}_{\tilde{\tau}} X^I = X_{\tilde{\tau}}^I + \Gamma_{JK}^I \phi_{\tilde{\tau}}^J X^K$ . As such, we see that the mass  $m_\phi$  drops out of the field equations. In particular, this means that the solution for  $\mathcal{H}$  as a function of  $\tilde{\tau}$  will be independent of  $m_\phi$ . If we then consider the definition of the  $e$ -folding number, we have

$$N = \int_{t_*}^t H dt = \int_{\tilde{\tau}_*}^{\tilde{\tau}} \mathcal{H} d\tilde{\tau}, \quad (4.6)$$

from which we conclude that the  $e$ -folding number is independent of the overall mass scale  $m_\phi$ . This in turn means that the derivatives of  $N$ , required in calculating  $\mathcal{P}_\zeta$ ,  $n_s$ ,  $r$  and  $f_{NL}$ , will also be independent of  $m_\phi$ . Given the expressions for  $n_s$ ,  $r$  and  $f_{NL}$ , we thus find that they are all independent of  $m_\phi$ . The only observable that depends on  $m_\phi$  is  $\mathcal{P}_\zeta$ , as this depends on the overall normalization of  $H_*^2$ .<sup>5</sup> Explicitly, we have

$$\mathcal{P}_\zeta(k) = m_\phi^2 \left( \frac{\mathcal{H}_*}{2\pi} \right)^2 \mathcal{G}_*^{IJ} N_{,I} N_{,J}, \quad (4.7)$$

which means that we are able to determine the quantity  $\mathcal{P}_\zeta/m_\phi^2$  without knowing  $m_\phi$ .

Using this new parameterization, the free parameters of the theory (assuming slow-roll at horizon crossing) are  $m_\phi$ ,  $R_{\text{mass}}$ ,  $\phi_*$  and  $\chi_*$ . We will now consider how the inflationary dynamics and predictions for  $\zeta$  depend on these parameters.

<sup>5</sup>Another way to see the independence of  $m_\phi$  is to write the field equations of motion directly in terms of the time parameter  $N$ . On doing so, the potential only appears in the combination  $V_{,I}/V$ , meaning that the overall factor of  $m_\phi^2$  drops out.

## Background trajectories

In light of the preceding discussion, we see that the shape of trajectories in field space will be independent of  $m_\phi$ . As such, the only remaining parameters are  $R_{\text{mass}}$ ,  $\phi_*$  and  $\chi_*$ . Broadly speaking, we are interested in the three regimes  $R_{\text{mass}} > 1$ ,  $R_{\text{mass}} \sim 1$  and  $R_{\text{mass}} < 1$ , and in Fig. 1 we plot example trajectories for the representative values  $R_{\text{mass}} = 5, 1, 1/5$ . In each case we consider the three sets of initial conditions  $(\phi_*/M_{pl}, \chi_*/M_{pl}) = (6, 3)$ ,  $(\phi_*/M_{pl}, \chi_*/M_{pl}) = (5, 3)$  and  $(\phi_*/M_{pl}, \chi_*/M_{pl}) = (6, 1.5)$ , and each trajectory is evolved until inflation ends. When interpreting the trajectories, one has to be careful to recall that it is not only the potential shape that is important, as the effect of the non-flat field space must also be taken into account. In this model, for example, we have  $\mathcal{G}^{\chi\chi} = e^{2\alpha\phi}$ . Given that the slow-roll equation of motion for  $\chi$  takes the form  $3H\dot{\chi} \simeq -\mathcal{G}^{\chi\chi}V_{,\chi}$ , we can expect that for super-Planckian values of  $\phi$  the velocity is enhanced compared to what we would naively expect from the gradient of the potential alone. Nevertheless, the trajectories in Fig. 1 qualitatively agree with our naive expectation.

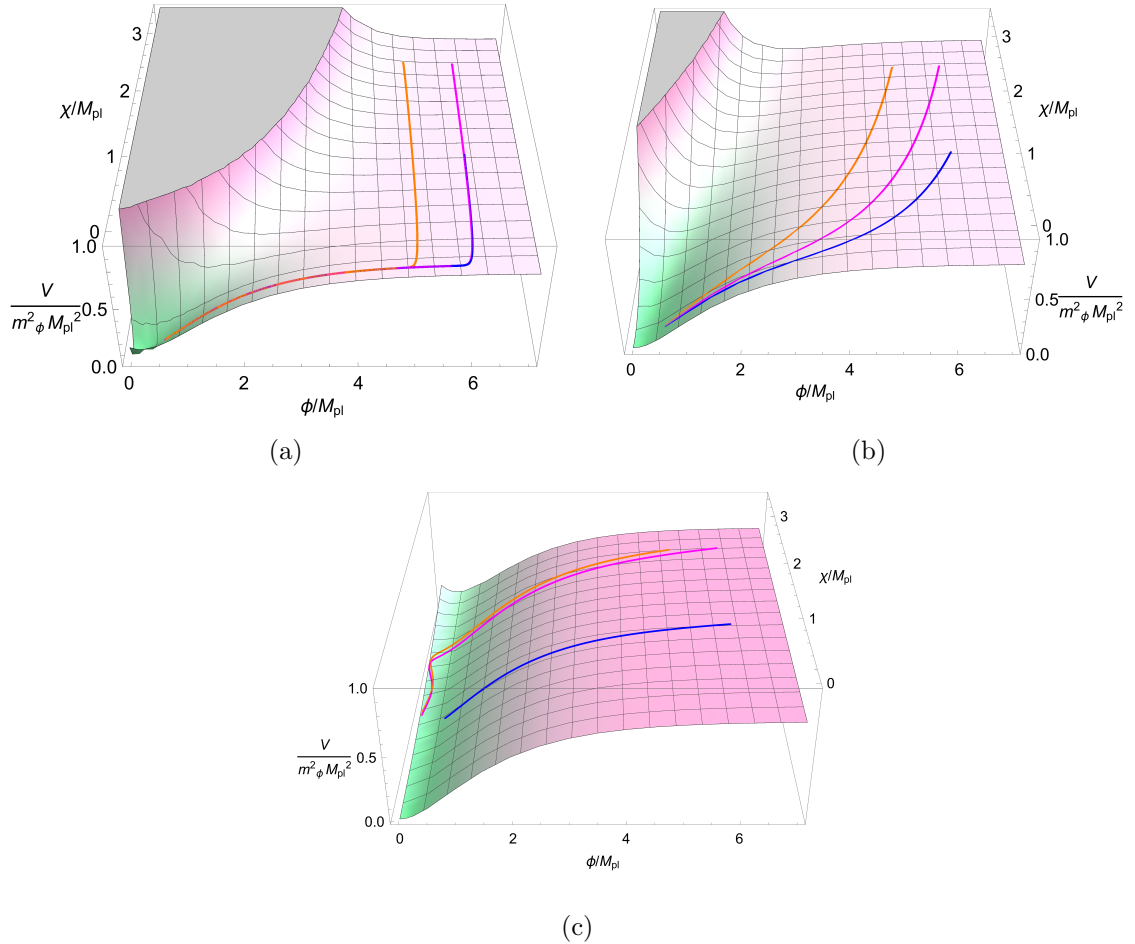


**Figure 1:** Examples trajectories for three different values of  $R_{\text{mass}}$ . We show the cases a)  $R_{\text{mass}} = 5.0$ , b)  $R_{\text{mass}} = 1.0$ , and c)  $R_{\text{mass}} = 0.2$ . For each value of  $R_{\text{mass}}$  three trajectories are plotted, with the initial conditions given as  $(\phi_*/M_{pl}, \chi_*/M_{pl}) = (6.0, 3.0)$  (magenta line),  $(\phi_*/M_{pl}, \chi_*/M_{pl}) = (5.0, 3.0)$  (orange line) and  $(\phi_*/M_{pl}, \chi_*/M_{pl}) = (6.0, 1.5)$  (blue line).

In the case  $R_{\text{mass}} = 5$  we find that the trajectories first rapidly evolve in the  $\chi$  direction, with most of inflation then taking place as the trajectory proceeds along the local minimum at  $\chi = 0$ . Given that the potential reduces to the single-field  $R^2$  potential at  $\chi = 0$ , we expect the last stage of inflation to be indistinguishable from the original  $R^2$  model. At the level of perturbations, as the trajectory evolves along the local minimum we expect that  $\zeta$  should be conserved and that isocurvature perturbations will decay, such that an adiabatic limit is approached. Recall that in the original  $R^2$  inflation model approximately 60  $e$ -foldings of inflation are obtained by taking  $\phi_*/M_{\text{pl}} \simeq 5.5$ . As such, in the large  $R_{\text{mass}}$  limit, if we take any set of initial conditions with  $\phi_*/M_{\text{pl}} \gtrsim 5.5$ , the final stage of inflation along  $\chi = 0$  will constitute the whole observable part of inflation, and we thus expect that predictions for  $\zeta$  and its statistical properties will be indistinguishable from the original  $R^2$  model.

In the case  $R_{\text{mass}} = 1$ , the trajectories are less trivial, in the sense that they continue to turn throughout the evolution. Correspondingly, we expect that  $\zeta$  will continue to evolve throughout inflation. It is in this parameter region that an adiabatic limit may not be reached by the end of inflation, and  $\zeta$  may continue to evolve through the (p)reheating epoch. If this is the case, then the correlation functions of  $\zeta$  that we find at the end of inflation should not be directly compared with observations.

Finally, in the case  $R_{\text{mass}} = 1/5$ , the trajectories are again as expected, with essentially two stages of inflation taking place. Initially the trajectories evolve in the  $\phi$  direction, with the potential profile in the  $\phi$  direction being very similar to that of the original  $R^2$  inflation model. In the cases of the orange and magenta trajectories, they then turn and inflation proceeds as they evolve essentially in the  $\chi$  direction but while oscillating about the local minimum located close to but not exactly at  $\phi = 0$ . For this choice of  $R_{\text{mass}}$ , these trajectories do not appear to fully relax to the bottom of the local minimum before the end of inflation, and so we might expect that  $\zeta$  is still evolving. In the case of the blue trajectory, due to the smaller initial position  $\chi_*/M_{\text{pl}} = 1.5$ , we find that there is no second stage of inflation driven by the  $\chi$  field.

A feature that it is common to all choices of  $R_{\text{mass}}$  is that for  $\chi = 0$  both the potential and  $V_{,\phi}$  reduce to those of  $R^2$  inflation, while  $V_{,\chi} = 0$ . Consequently, trajectories with  $\chi_* = 0$  will evolve purely in the  $\phi$  direction, and we expect that predictions for  $\zeta$  will coincide with those of  $R^2$  inflation.

As we move to non-zero values of  $\chi$ , deviations from the  $R^2$  potential depend on  $R_{\text{mass}}$ ,  $\phi$  and  $\chi$ . For super-Planckian values of  $\phi$  satisfying  $2\alpha\phi \gg 1$ , such that  $e^{-2\alpha\phi} \ll 1$ , deviations from the  $R^2$  potential are suppressed by a factor of  $e^{-4\alpha\phi}$ , and will therefore be negligible for sufficiently large values of  $\phi$ . This feature can be seen in all panels of Fig. 1. In order for the  $\chi$ -field contribution to the potential to dominate at some super-Planckian value of  $\phi$ , one would require  $R_{\text{mass}}^2 \chi^2 \gg 3M_{\text{pl}}^2 e^{4\alpha\phi}/2$ , i.e.  $R_{\text{mass}}$  or  $\chi$  must be very large. However, in such a parameter region we find that  $\epsilon_\phi \equiv M_{\text{pl}}^2 (V_{,\phi}/V)^2/2 \simeq 8M_{\text{pl}}^2 \alpha^2 > 1$ , such that  $\epsilon_V = \epsilon_\phi + \epsilon_\chi > 1$ , where  $\epsilon_\chi \equiv M_{\text{pl}}^2 e^{2\alpha\phi} (V_{,\chi}/V)^2/2$ , i.e. the slow-roll approximation breaks down.

Note that although the potential reduces to  $m_\chi^2 \chi^2/2$  if we take  $\phi = 0$ , due to the interaction term we do not have  $V_{,\phi} = 0$  when  $\phi = 0$ . As such, even if we start with  $\phi_* = 0$ , we do not necessarily obtain chaotic inflation along the  $\chi$  direction. Indeed,  $\dot{\phi}$  is positive along the axis  $\phi = 0$ , and if we calculate  $\epsilon_\phi$  we again find  $\epsilon_\phi = 8M_{\text{pl}}^2 \alpha^2 > 1$ , such that  $\epsilon_V > 1$  and the slow-roll approximation is violated. Nevertheless, in the limit  $R_{\text{mass}} \ll 1$ , with appropriate initial conditions we do find that the final stages of inflation essentially coincide with quadratic chaotic inflation driven by the  $\chi$  field. As can be seen in the third panel of Fig 1, for small values of  $R_{\text{mass}}$  and sufficiently super-Planckian initial conditions for

$\phi$  and  $\chi$ , we obtain two stages of inflation. The first stage is driven by  $\phi$ , and once  $\phi$  reaches its minimum the second stage is driven essentially by  $\chi$ . The minimum of the potential in the  $\phi$  direction lies on the curve defined by

$$\frac{2}{3}R_{\text{mass}}^2 \frac{\chi^2}{M_{\text{pl}}^2} = e^{2\alpha\phi} - 1. \quad (4.8)$$

As such, if  $R_{\text{mass}}$  is small enough to ensure that  $R_{\text{mass}}\chi/M_{\text{pl}} \ll \sqrt{3/2}$ , we find that the minimum lies very close to the  $\chi$  axis, with  $\phi/M_{\text{pl}} \ll \sqrt{3/2}$ . In the same limit  $R_{\text{mass}}\chi/M_{\text{pl}} \ll \sqrt{3/2}$ , we find that along the minimum with respect to  $\phi$  the potential and its derivative with respect to  $\chi$  are approximately given as

$$V|_{V,\phi=0} \simeq \frac{1}{2}m_\chi^2\chi^2, \quad V_{,\chi}|_{V,\phi=0} \simeq m_\chi^2\chi, \quad (4.9)$$

i.e. they coincide with the case of a quadratic mass term for the  $\chi$  field. Consequently, in the limit  $R_{\text{mass}} \ll 1$ , or more precisely  $R_{\text{mass}} \ll \sqrt{3/2}M_{\text{pl}}/\chi_*$ , once the  $\phi$  field has evolved to its minimum we expect quadratic chaotic inflation driven by  $\chi$  to take place. If we require that this stage of chaotic inflation lasts for approximately 60  $e$ -foldings, then this means we require  $\chi_* \simeq 15.5M_{\text{pl}}$ , which in turn gives the condition  $R_{\text{mass}} \ll \sqrt{3/2}/15.5 \simeq 0.08$ . In analogy with the large  $R_{\text{mass}}$  limit, we find that for  $R_{\text{mass}} \ll 0.08$  the whole of the observable period of inflation will essentially coincide with quadratic chaotic inflation driven by  $\chi$  if we take any initial conditions with  $\chi_* \gtrsim 15.5M_{\text{pl}}$ . At the level of perturbations, in analogy with the large  $R_{\text{mass}}$  case, as the trajectory evolves along the the local minimum close to  $\phi = 0$  we expect that  $\zeta$  will be conserved and that isocurvature perturbations decay, such that an adiabatic limit is approached.

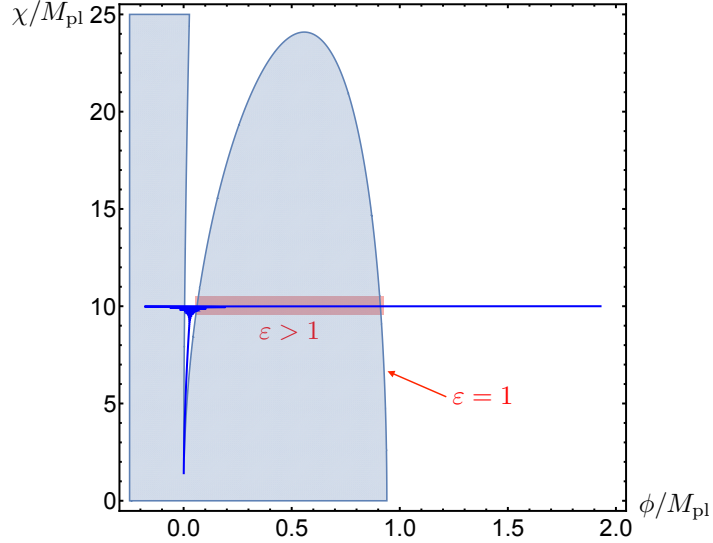


**Figure 2:** An example trajectory for  $R_{\text{mass}} = 0.02$  and  $(\phi_*/M_{\text{pl}}, \chi_*/M_{\text{pl}}) = (2.0, 10.0)$ . The region with  $\epsilon_V > 1$  is shaded in blue. The trajectory consists of two inflationary stages separated by a non-inflationary stage.

Given that the mass ratio  $R_{\text{mass}} = 0.2$  considered in Fig. 1 is not so small, in Fig. 2 we plot an example trajectory for the case  $R_{\text{mass}} = 0.02$  and the initial conditions  $(\phi_*/M_{\text{pl}}, \chi_*/M_{\text{pl}}) =$



(2.0, 10.0) . We also show the region where  $\epsilon_V > 1$ . Similar to the case  $R_{\text{mass}} = 0.2$  considered in Fig. 1, the trajectory first evolves in the  $\phi$  direction and the potential profile essentially coincides with  $R^2$  inflation. Intermediately, when  $\phi$  drops below  $M_{pl}$ , one thus finds that  $\epsilon_V$  becomes greater than unity and inflation temporarily ceases. However, once the trajectory reaches the local minimum,  $\epsilon_V$  once again becomes less than unity and inflation recommences, with the subsequent trajectory evolving essentially in the  $\chi$  direction. It is thus important when considering small values of  $R_{\text{mass}}$  that we do not terminate our integration of the trajectory prematurely, in order not to miss the second stage of inflation. Note that there is a period during which the  $\phi$  field oscillates about its minimum, and during this period one might expect the  $\phi$  field to decay into any matter fields to which it is coupled, including the  $\chi$  field. Indeed, due to the non-minimal coupling of  $\phi$  to the Ricci scalar in the Jordan frame, we expect there to at least be gravitationally induced couplings between  $\phi$  and any other matter fields present, see e.g. [41, 42]. However, in the following we neglect the possible decay of the  $\phi$  field, postponing a careful consideration of this effect to future work.

### Evolution of perturbations

Having given some example background trajectories, we now consider the evolution of  $\zeta$ , or more precisely its correlation functions. As discussed above, in single field inflation we know that  $\zeta$  is conserved on superhorizon scales, while in multi-field inflation it is sourced by isocurvature perturbations if the trajectory in field space deviates from a geodesic, see e.g. [25, 26].

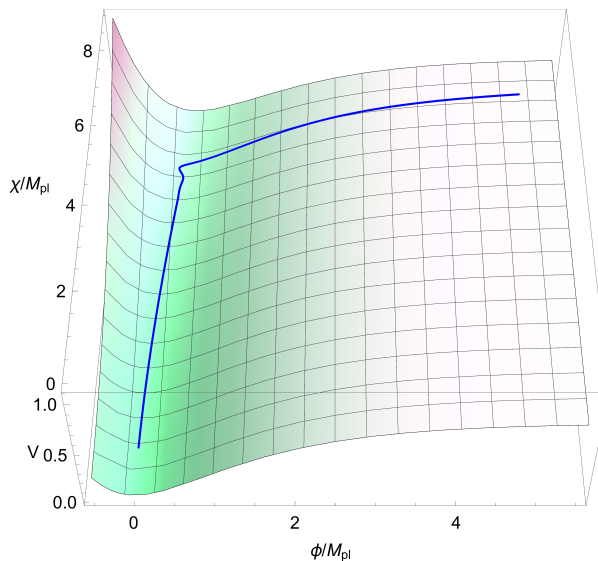


**Figure 3:** An example trajectory with  $R_{\text{mass}} = 0.1$  and initial conditions  $(\phi_*/M_{pl}, \chi_*/M_{pl}) = (5.0, 8.0)$ . Inflation lasts for a total of 58  $e$ -foldings.

Perhaps the most interesting evolution of  $\zeta$  and its correlation functions is observed in the case of small  $R_{\text{mass}}$ . As an example, we consider the parameters  $R_{\text{mass}} = 0.1$  and  $(\phi_*/M_{pl}, \chi_*/M_{pl}) = (5, 8)$ . The background trajectory for this choice of parameters is shown in Fig. 3. Given that  $R_{\text{mass}} \ll 1$ , we see that the trajectory first evolves in the  $\phi$  direction, before moving along the local minimum that runs almost parallel to the  $\chi$  axis. In total there

are approximately 60  $e$ -foldings of inflation, with the turn occurring at  $N \sim 45$ . In the left panel of Fig. 4 we plot the evolution of the power spectrum, normalised by the final value. As expected, it remains constant for the first 40  $e$ -folds, and is then sourced by isocurvature modes as the trajectory turns at around  $N \sim 45$ . Given the relatively large mass hierarchy,  $\mathcal{P}_\zeta$  is seen to oscillate as the trajectory oscillates about the local minimum, before again approaching a constant as an essentially single-field limit is reached.

In the right panel of Fig. 4 we show the evolution of  $f_{NL}$  for the same trajectory. Up until the turn it is negligibly small, with  $f_{NL} \sim \mathcal{O}(10^{-2})$ . During the turn and subsequent oscillations we find that  $f_{NL}$  also oscillates, with a peak amplitude of  $f_{NL} \simeq 0.35$ . In the final stage, however,  $f_{NL}$  relaxes back down to an unobservably small value of  $\mathcal{O}(10^{-2})$ . The behaviour of the power spectrum and  $f_{NL}$  in this example are qualitatively very similar to that observed in double quadratic inflation models, see e.g. [36, 43, 44] and references therein.

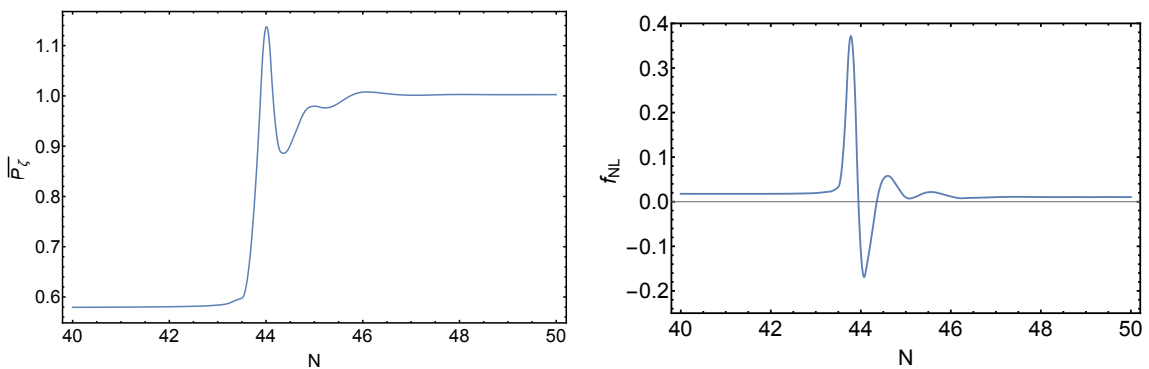


**Figure 4:** Evolution of the normalised power spectrum  $\overline{\mathcal{P}}_\zeta = P_\zeta(N)/P_\zeta(N_{\text{final}})$  (left panel) and  $f_{NL}$  (right panel) for the example trajectory plotted in Fig. 3.

We have also considered the evolution of  $\mathcal{P}_\zeta$  and  $f_{NL}$  in the other regimes  $R_{\text{mass}} > 1$  and  $R_{\text{mass}} \sim 1$ . For trajectories with  $R_{\text{mass}} > 1$ , such as those shown in the first panel of Fig. 1, due to the fact that the trajectories quickly evolve to the  $\phi$  axis and reach an effectively single-field trajectory along the  $\phi$  axis, we find that  $\mathcal{P}_\zeta$  and  $f_{NL}$  also quickly reach constant values, with  $f_{NL} \sim \mathcal{O}(10^{-2})$ . Note that the background trajectories shown in the first panel of Fig. 1 do not oscillate about the  $\phi$  axis, and correspondingly we find that  $\mathcal{P}_\zeta$  and  $f_{NL}$  also do not oscillate before settling to their constant values. For trajectories with  $R_{\text{mass}} \sim 1$ , such as those shown in the second panel of Fig. 1, we find that the evolution of  $\mathcal{P}_\zeta$  and  $f_{NL}$  is much more gradual, with  $f_{NL}$  remaining  $\mathcal{O}(10^{-2})$  throughout the evolution.

### Exploring and constraining parameter space

Having looked at representative example trajectories in the three regimes  $R_{\text{mass}} < 1$ ,  $R_{\text{mass}} \sim 1$  and  $R_{\text{mass}} > 1$ , we now proceed to put constraints on the parameters  $m_\phi$  and  $R_{\text{mass}}$ . In doing so we consider thirty-one different mass ratios in the range  $10^{-3} \leq R_{\text{mass}} \leq 10^3$ , distributed evenly over  $\log R_{\text{mass}}$ . For each value of  $R_{\text{mass}}$  we then consider a  $50 \times 50$  grid of initial conditions  $(\phi_*, \chi_*)$ , with  $\phi_*$  spanning the range  $0 \leq \phi_* \leq 6M_{pl}$  and  $\chi_*$  spanning the range  $0 \leq \chi_* \leq 16M_{pl}$ .<sup>6</sup> Next we neglect any points on the grid for which either  $\epsilon_V > 1$

<sup>6</sup>From our knowledge of the  $R^2$  and quadratic chaotic inflation models, we know that taking  $\phi_* > 6$  or  $\chi_* > 16$  will always give  $N > 60$ , but observationally we are only interested in the last 60  $e$ -folds of inflation.

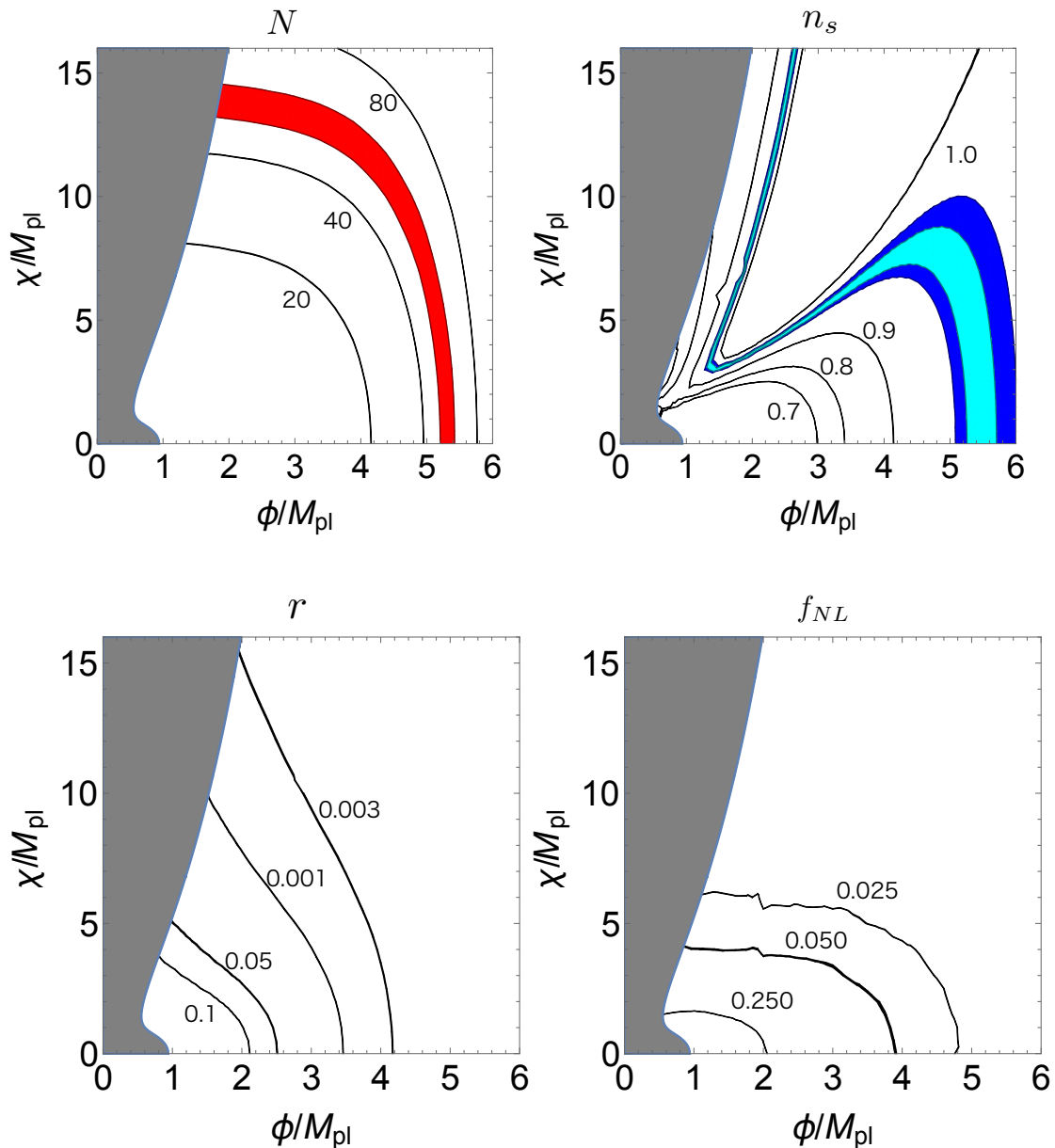


**Figure 5:** Predictions in the  $\phi_*$ - $\chi_*$  plane for the  $e$ -folding number  $N$  (upper left), spectral tilt  $n_s$  (upper right), tensor-to-scalar ratio  $r$  (lower left) and non-Gaussianity parameter  $f_{\text{NL}}$  (lower right) for the case  $R_{\text{mass}} = 1.0$ . The red shaded region in the upper left plot shows the initial conditions for which  $50 < N < 60$ . The light blue (dark blue) shaded region in the upper right plot indicates the range of initial conditions for which  $n_s$  lies within  $1\text{-}\sigma$  ( $2\text{-}\sigma$ ) of the observed value. The grey shaded region in all plots corresponds to where  $\epsilon_V > 1$ .

or  $|\eta_V| > 1$ , i.e. we require that the slow-roll approximation is valid at the horizon-crossing time. For the remaining points we are then able to determine  $N$ ,  $\mathcal{P}_\zeta/m_\phi^2$ ,  $n_s$ ,  $r$  and  $f_{\text{NL}}$

---

Hence our choice of maximum  $\phi_*$  and  $\chi_*$ .

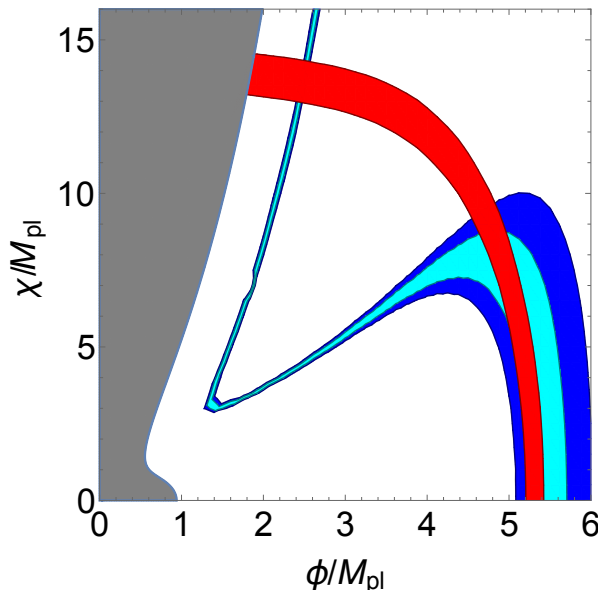


**Figure 6:** Combined constraints in the  $\phi_*$ - $\chi_*$  plane for the case  $R_{\text{mass}} = 1$ . The red shaded region corresponds to the constraint  $50 < N < 60$ , while the light- and dark-blue regions correspond to the 1- and 2- $\sigma$  observational constraints on  $n_s$  given at the end of Sec. 3. Predictions for  $r$  and  $f_{NL}$  are consistent with observations for all sets of initial conditions. The grey shaded region corresponds to where  $\epsilon_V > 1$ .

without needing to specify  $m_\phi$ . Neglecting points that do not give  $50 < N < 60$ , for each of the remaining points we perform a chi-squared analysis to determine the range of  $m_\phi$  for which the predictions for  $\mathcal{P}_\zeta$ ,  $n_s$ ,  $r$  and  $f_{NL}$  lie within 1- and 2- $\sigma$  of the observed values summarised at the end of Sec. 3. At this point, for every observationally allowed set of initial conditions  $(\phi_*, \chi_*)$  we have a maximum and minimum allowed  $m_\phi$ . To find the overall maximum and minimum allowed values of  $m_\phi$  for a given  $R_{\text{mass}}$ , we must then take the maximum of all the maxima and the minimum of all the minima. Note that for any value of  $R_{\text{mass}}$  we are guaranteed to find a non-vanishing allowed range of  $m_\phi$ , as we will always recover the predictions of  $R^2$  inflation if we take  $\chi_* = 0$ .

As an example, in Fig. 5 we show the predictions for  $N$ ,  $n_s$ ,  $r$  and  $f_{NL}$  in the  $\phi_*$ - $\chi_*$  plane for the case  $R_{\text{mass}} = 1$ . In the plot of  $N$  we highlight in red the region for which  $50 < N < 60$ . Similarly, in the plot of  $n_s$  we highlight in light- and dark-blue the regions that fall within 1- and 2- $\sigma$  of the observed value. For all values of  $\phi_*$  and  $\chi_*$  we find that  $r$  and  $f_{NL}$  are consistent with observational constraints. In Fig. 6 we combine the constraints coming from  $N$  and  $n_s$ , which allows us to determine the region in the  $\phi_*$ - $\chi_*$  plane in which the horizon exit point must lie. The intersection of the red shaded region with the  $\phi$  axis corresponds to the initial conditions for  $R^2$  inflation. As we move away from the  $\phi$  axis we see that there is quite an extended region that remains in agreement with observations. Interestingly, there is another small allowed region towards the top left-hand corner of the  $\phi_*$ - $\chi_*$  plane.

The obtained constraints on  $m_\phi$  as a function of  $R_{\text{mass}}$  are shown in Fig. 7. In the limits of both small and large  $R_{\text{mass}}$  we find that the allowed range is consistent with that of  $R^2$

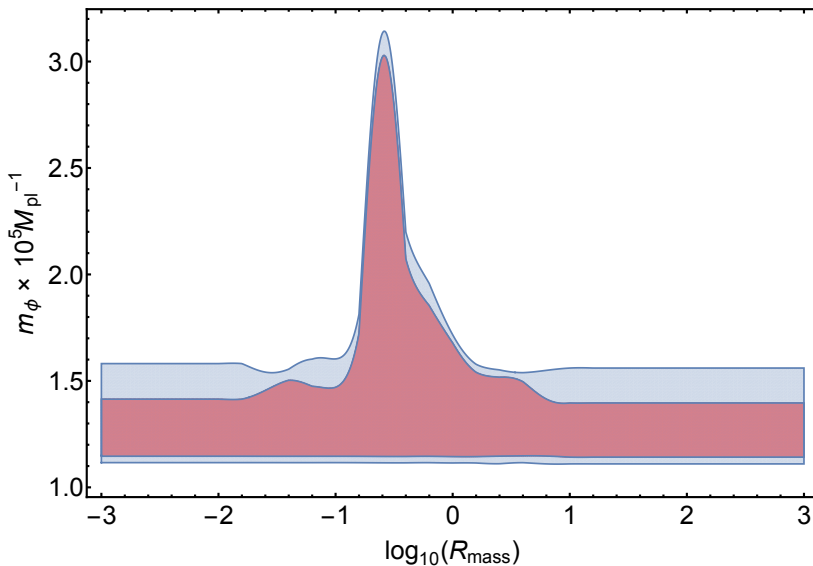


**Figure 7:** Allowed regions in the  $R_{\text{mass}}-m_\phi$  plane at 1- $\sigma$  (red shaded region) and 2- $\sigma$  (blue shaded region).

inflation, for which slow-roll estimates give  $m_\phi \simeq (1.2-1.4) \times 10^{-5} M_{pl}$  for  $N = 50-60$ . In the large  $R_{\text{mass}}$  limit this has a relatively simple interpretation. As the  $\chi$  field becomes more massive one approaches a limit in which all slow-roll trajectories satisfying  $\epsilon_V, |\eta_V| \ll 1$  at horizon crossing and giving  $50 < N < 60$  correspond to effectively single-field trajectories that evolve along the  $\phi$  axis, where the potential reduces to that of  $R^2$  inflation. We can see from Fig. 7 that such a limit is reached for  $R_{\text{mass}} \gtrsim 10$ . In the small  $R_{\text{mass}}$  limit the situation is less clear. The fact that the allowed range of  $m_\phi$  approaches a constant can be understood as follows. So long as  $R_{\text{mass}}$  is smaller than some critical value — which our results suggest is around  $R_{\text{mass}} \simeq 10^{-2}$  — one finds that for a given set of initial conditions the last 60  $e$ -foldings of inflation is well approximated by a stage of  $R^2$  inflation followed by a stage of quadratic chaotic inflation, as was observed in Fig. 2. The fact that the allowed range of  $m_\phi$  coincides with that of  $R^2$  inflation, however, is not so obvious. As  $\chi_*$  is increased from 0 to  $16M_{pl}$  (and  $\phi_*$  is correspondingly adjusted to give the desired number of  $e$ -foldings), we expect that predictions for  $\mathcal{P}_\zeta, r, n_s$  and  $f_{NL}$  will interpolate between those of  $R^2$  inflation and those of quadratic chaotic inflation. While the latter are ruled out by observations, one might naively expect that intermediately there are values of  $\chi_*$  that give predictions deviating from  $R^2$  inflation but still in agreement with observations, which in turn would naively alter the allowed range of  $m_\phi$ . However, our results suggest that the allowed range of  $m_\phi$  is essentially unaffected.

For intermediate values of  $R_{\text{mass}}$  the obtained bounds on  $m_\phi$  are found to deviate from those of  $R^2$  inflation. As we can see in Fig. 7, the allowed range of  $m_\phi$  has a peak of  $m_\phi \simeq 3 \times 10^{-5} M_{pl}$  at around  $\log_{10}(R_{\text{mass}}) \simeq -0.5$  ( $R_{\text{mass}} \simeq 0.3$ ). However, one must bear in mind that for some of the trajectories in this parameter range an adiabatic limit will not have been reached by the end of inflation. As such, it may be that the constraints in this region would change if effects of the (p)reheating epoch were taken into account.

Using the definition of  $R_{\text{mass}}$ , we can use the above constraints on  $m_\phi$  to also put bounds on  $m_\chi$  as a function of  $R_{\text{mass}}$ . The results are shown in Fig. 8a. Similarly, recall that in the Jordan frame representation of this model one has the parameter  $\mu$  instead of  $m_\phi$ , see eq. (2.1). Given that these two parameters are related as  $m_\phi^2 = M_{\text{pl}}^2/(6\mu)$ , we can re-express our constraints on  $m_\phi$  as constraints on  $\mu$ , and the results are shown in Fig. 8b. In the original  $R^2$  inflation model, slow-roll estimates determine that in order to satisfy observational constraints one requires  $\mu \simeq (0.9\text{--}1.2) \times 10^9$  for  $N=50\text{--}60$  [45, 46], which is consistent with our constraints. In the multi-field extension of  $R^2$  inflation that we have considered, we find the allowed range of  $\mu$  to be  $\mu \simeq (0.2\text{--}1.3) \times 10^9$ .

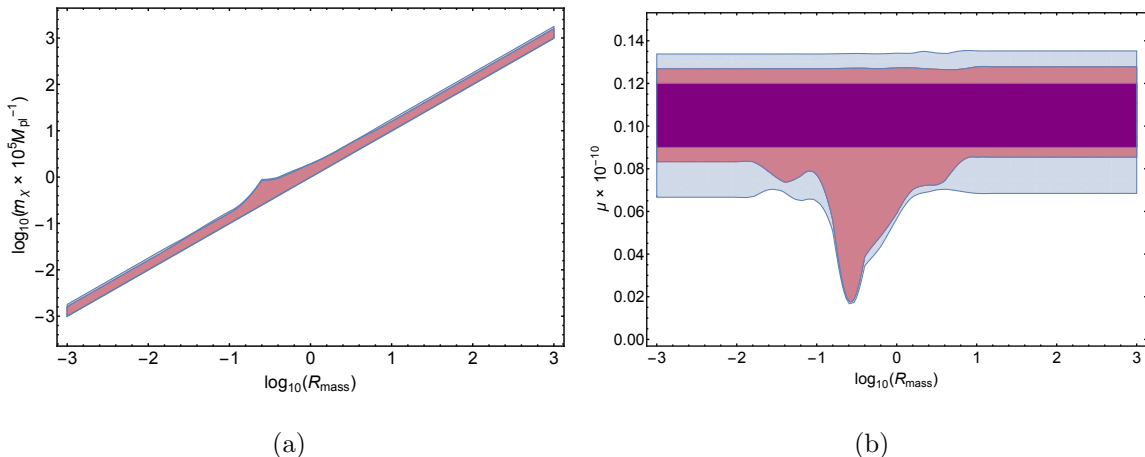


**Figure 8:** (a) Allowed regions in the  $R_{\text{mass}}-m_\chi$  plane at 1- $\sigma$  (red shaded region) and 2- $\sigma$  (blue shaded region). (b) Allowed regions in the  $R_{\text{mass}}-\mu$  plane at 1- $\sigma$  (red shaded region) and 2- $\sigma$  (blue shaded region). The purple-shaded region shows  $\mu = (0.9\text{--}1.2) \times 10^9$ , which corresponding to the case of the original  $R^2$  inflation model with  $N = 50\text{--}60$ .

## 5 Summary

In this paper we have considered a two-field inflation model based on a simple multi-field extension of  $R^2$  inflation. In addition to a term proportional to  $R^2$ , the Jordan frame action contains a canonical scalar field  $\chi$  with quadratic mass term. On re-writing the model as a scalar-tensor theory and making a conformal transformation into the Einstein frame, the model takes the form of a two-field inflation model with a non-flat field space as shown in eq. (2.6). The first field,  $\phi$ , corresponds to the additional degree of freedom associated with the  $R^2$  term in the original action and is often referred to as the scalaron. This field has a canonical kinetic term and its potential takes on the same form as in the original  $R^2$  inflation model, approaching a constant for super-Planckian values of  $\phi$ . The second field,  $\chi$ , on the other hand, has a non-canonical kinetic term that depends exponentially on  $\phi$ , and its quadratic mass term similarly contains an exponential coupling with  $\phi$ .

Assuming that the slow-roll approximation is valid at horizon crossing, such that only the initial field positions have to be specified in solving for the inflationary dynamics, the four free parameters of the model are  $m_\phi$ ,  $R_{\text{mass}} = m_\chi/m_\phi$ ,  $\phi_*$  and  $\chi_*$ . In Sec. 4 we have explored how the inflationary dynamics and predictions for the correlation functions of  $\zeta$  depend on these four parameters, both qualitatively and quantitatively.

For  $R_{\text{mass}} \gtrsim 10$  we find that all slow-roll trajectories satisfying  $\epsilon_V, |\eta_V| \ll 1$  at horizon crossing and giving  $50 < N < 60$  follow an effectively single-field trajectory evolving along the local minimum of the potential at  $\chi = 0$ . Given that the potential coincides with that of the original  $R^2$  inflation model along  $\chi = 0$ , the predictions for  $\zeta$  and its correlation functions also coincide with the original model. In this region of parameter space observational constraints give  $m_\phi \simeq (1.1\text{--}1.6) \times 10^{-5} M_{pl}$  at  $2\text{-}\sigma$ .

For  $R_{\text{mass}} \lesssim 10^{-2}$  we find that inflationary trajectories consist of a stage of  $R^2$  inflation driven by  $\phi$  followed by a stage of quadratic chaotic inflation driven by  $\chi$ . How the last observable 60  $e$ -foldings of inflation are divided between these two stages depends on the initial conditions, and the predictions for  $\zeta$  and its correlation functions thus range from those of  $R^2$  inflation to those of quadratic chaotic inflation. Interestingly, however, we find that the final constraints on  $m_\phi$  are very similar to those obtained in the large  $R_{\text{mass}}$  limit, namely they essentially coincide with the limits on  $m_\phi$  obtained in the original  $R^2$  model.

Finally, in the parameter region  $R_{\text{mass}} \sim 1$ , we find that the constraints on  $m_\phi$  are less tight, with  $m_\phi \simeq (1.1\text{--}3.2) \times 10^{-5} M_{pl}$  at  $2\text{-}\sigma$ . Here it is less easy to interpret the results, as the inflationary trajectories are truly multi-field in nature, with both  $\phi$  and  $\chi$  evolving throughout inflation in many cases and the dynamics very much depending on the initial conditions. Nevertheless, one can see that the net result of these multi-field effects is to increase the allowed range of  $m_\phi$  as compared to the original  $R^2$  model, and in particular to allow for larger values of  $m_\phi$ .

One issue that we have not fully addressed in this paper is the possibility that  $\zeta$  may continue to evolve after the end of inflation. If an adiabatic limit is not reached by the end of inflation then one should continue to follow the evolution of  $\zeta$  through (p)reheating and until an adiabatic limit is reached. It is only the final  $\zeta$  that should then be compared with observations. In the cases  $R_{\text{mass}} \gg 1$  and  $R_{\text{mass}} \ll 1$  the issue is naively not important, as we expect an adiabatic limit to be reached before the end of inflation for most inflationary trajectories. For  $R_{\text{mass}} \sim 1$ , however, this is no longer the case, and so post-inflationary evolution of  $\zeta$  may affect the constraints on  $m_\phi$  in this region. We hope to address this issue in future work.

## Acknowledgments

We would like to thank M. Karčiauskas for valuable discussions in the early stage of this work. This work was partially supported by JSPS Core-to-Core Program, Advanced Research Networks (T.M.), JSPS KAKENHI Grant Nos. 26247042, and JP1701131 (K.K.), and MEXT KAKENHI Grant Nos. JP15H05889, and JP16H0877 (K.K.). T.M. thanks the members of the ICG Group at Portsmouth for their hospitality.

## Appendix: Explicit form of $\Gamma_{JK}^I$

According to the action (2.6), the metric of the field space  $\mathcal{G}_{IJ}$  and its inverse are given as

$$\mathcal{G}_{IJ} = \begin{pmatrix} 1 & 0 \\ 0 & e^{-2\alpha\phi} \end{pmatrix}, \quad \mathcal{G}^{IJ} = \begin{pmatrix} 1 & 0 \\ 0 & e^{2\alpha\phi} \end{pmatrix}. \quad (\text{A.1})$$

Using the definition of the Christoffel symbols

$$\Gamma_{JK}^I = \frac{1}{2} \mathcal{G}^{IL} (\partial_J \mathcal{G}_{LK} + \partial_K \mathcal{G}_{JL} - \partial_L \mathcal{G}_{JK}), \quad (\text{A.2})$$

we find the various components to be given as

$$\Gamma_{\chi\chi}^{\chi} = 0, \quad \Gamma_{\chi\phi}^{\chi} = \Gamma_{\phi\chi}^{\chi} = -\alpha, \quad \Gamma_{\phi\phi}^{\chi} = 0, \quad (\text{A.3})$$

$$\Gamma_{\phi\phi}^{\phi} = 0, \quad \Gamma_{\phi\chi}^{\phi} = \Gamma_{\chi\phi}^{\phi} = 0, \quad \Gamma_{\chi\chi}^{\phi} = \alpha e^{-2\alpha\phi}. \quad (\text{A.4})$$

## References

- [1] PLANCK collaboration, P. A. R. Ade et al., *Planck 2015 results. XX. Constraints on inflation*, *Astron. Astrophys.* **594** (2016) A20, [[1502.02114](#)].
- [2] J. M. Maldacena, *Non-Gaussian features of primordial fluctuations in single field inflationary models*, *JHEP* **05** (2003) 013, [[astro-ph/0210603](#)].
- [3] SKA-JAPAN CONSORTIUM COSMOLOGY SCIENCE WORKING GROUP collaboration, D. Yamauchi et al., *Cosmology with the Square Kilometre Array by SKA-Japan*, *PoS DSU2015* (2016) 004, [[1603.01959](#)].
- [4] A. A. Starobinsky, *A New Type of Isotropic Cosmological Models Without Singularity*, *Phys. Lett.* **B91** (1980) 99–102.
- [5] R. Kallosh and A. Linde, *Superconformal generalizations of the Starobinsky model*, *JCAP* **1306** (2013) 028, [[1306.3214](#)].
- [6] C. van de Bruck and L. E. Paduraru, *Simplest extension of Starobinsky inflation*, *Phys. Rev.* **D92** (2015) 083513, [[1505.01727](#)].
- [7] J. Ellis, M. A. G. Garcia, D. V. Nanopoulos and K. A. Olive, *A No-Scale Inflationary Model to Fit Them All*, *JCAP* **1408** (2014) 044, [[1405.0271](#)].
- [8] J. Ellis, M. A. G. García, D. V. Nanopoulos and K. A. Olive, *Two-Field Analysis of No-Scale Supergravity Inflation*, *JCAP* **1501** (2015) 010, [[1409.8197](#)].
- [9] M. Sasaki and E. D. Stewart, *A General analytic formula for the spectral index of the density perturbations produced during inflation*, *Prog. Theor. Phys.* **95** (1996) 71–78, [[astro-ph/9507001](#)].
- [10] M. Sasaki and T. Tanaka, *Superhorizon scale dynamics of multiscalar inflation*, *Prog. Theor. Phys.* **99** (1998) 763–782, [[gr-qc/9801017](#)].
- [11] D. Wands, K. A. Malik, D. H. Lyth and A. R. Liddle, *A New approach to the evolution of cosmological perturbations on large scales*, *Phys. Rev.* **D62** (2000) 043527, [[astro-ph/0003278](#)].
- [12] D. H. Lyth, K. A. Malik and M. Sasaki, *A General proof of the conservation of the curvature perturbation*, *JCAP* **0505** (2005) 004, [[astro-ph/0411220](#)].
- [13] D. H. Lyth and Y. Rodriguez, *The Inflationary prediction for primordial non-Gaussianity*, *Phys. Rev. Lett.* **95** (2005) 121302, [[astro-ph/0504045](#)].
- [14] N. S. Sugiyama, E. Komatsu and T. Futamase,  *$\delta N$  formalism*, *Phys. Rev.* **D87** (2013) 023530, [[1208.1073](#)].
- [15] A. De Felice and S. Tsujikawa,  *$f(R)$  theories*, *Living Rev. Rel.* **13** (2010) 3, [[1002.4928](#)].
- [16] T. T. Nakamura and E. D. Stewart, *The Spectrum of cosmological perturbations produced by a multicomponent inflaton to second order in the slow roll approximation*, *Phys. Lett.* **B381** (1996) 413–419, [[astro-ph/9604103](#)].
- [17] J.-O. Gong and T. Tanaka, *A covariant approach to general field space metric in multi-field inflation*, *JCAP* **1103** (2011) 015, [[1101.4809](#)].
- [18] J. Elliston, D. Seery and R. Tavakol, *The inflationary bispectrum with curved field-space*, *JCAP* **1211** (2012) 060, [[1208.6011](#)].



- [19] D. I. Kaiser, E. A. Mazenc and E. I. Sfakianakis, *Primordial Bispectrum from Multifield Inflation with Nonminimal Couplings*, *Phys. Rev.* **D87** (2013) 064004, [[1210.7487](#)].
- [20] D. Seery and J. E. Lidsey, *Primordial non-Gaussianities from multiple-field inflation*, *JCAP* **0509** (2005) 011, [[astro-ph/0506056](#)].
- [21] D. H. Lyth and I. Zaballa, *A Bound concerning primordial non-Gaussianity*, *JCAP* **0510** (2005) 005, [[astro-ph/0507608](#)].
- [22] B. A. Bassett, S. Tsujikawa and D. Wands, *Inflation dynamics and reheating*, *Rev. Mod. Phys.* **78** (2006) 537–589, [[astro-ph/0507632](#)].
- [23] A. Naruko and M. Sasaki, *Conservation of the nonlinear curvature perturbation in generic single-field inflation*, *Class. Quant. Grav.* **28** (2011) 072001, [[1101.3180](#)].
- [24] X. Gao, *Conserved cosmological perturbation in Galileon models*, *JCAP* **1110** (2011) 021, [[1106.0292](#)].
- [25] C. Gordon, D. Wands, B. A. Bassett and R. Maartens, *Adiabatic and entropy perturbations from inflation*, *Phys. Rev.* **D63** (2001) 023506, [[astro-ph/0009131](#)].
- [26] D. Langlois and S. Renaux-Petel, *Perturbations in generalized multi-field inflation*, *JCAP* **0804** (2008) 017, [[0801.1085](#)].
- [27] C. van de Bruck, P. Dunsby and L. E. Paduraru, *Reheating and preheating in the simplest extension of Starobinsky inflation*, [1606.04346](#).
- [28] N. Deruelle and M. Sasaki, *Conformal equivalence in classical gravity: the example of 'Veiled' General Relativity*, *Springer Proc. Phys.* **137** (2011) 247–260, [[1007.3563](#)].
- [29] G. Domènech and M. Sasaki, *Conformal Frame Dependence of Inflation*, *JCAP* **1504** (2015) 022, [[1501.07699](#)].
- [30] N. Makino and M. Sasaki, *The Density perturbation in the chaotic inflation with nonminimal coupling*, *Prog. Theor. Phys.* **86** (1991) 103–118.
- [31] T. Chiba and M. Yamaguchi, *Extended Slow-Roll Conditions and Primordial Fluctuations: Multiple Scalar Fields and Generalized Gravity*, *JCAP* **0901** (2009) 019, [[0810.5387](#)].
- [32] J.-O. Gong, J.-c. Hwang, W.-I. Park, M. Sasaki and Y.-S. Song, *Conformal invariance of curvature perturbation*, *JCAP* **1109** (2011) 023, [[1107.1840](#)].
- [33] J. White, M. Minamitsuji and M. Sasaki, *Curvature perturbation in multi-field inflation with non-minimal coupling*, *JCAP* **1207** (2012) 039, [[1205.0656](#)].
- [34] J. White, M. Minamitsuji and M. Sasaki, *Non-linear curvature perturbation in multi-field inflation models with non-minimal coupling*, *JCAP* **1309** (2013) 015, [[1306.6186](#)].
- [35] T. Chiba and M. Yamaguchi, *Conformal-Frame (In)dependence of Cosmological Observations in Scalar-Tensor Theory*, *JCAP* **1310** (2013) 040, [[1308.1142](#)].
- [36] F. Vernizzi and D. Wands, *Non-gaussianities in two-field inflation*, *JCAP* **0605** (2006) 019, [[astro-ph/0603799](#)].
- [37] K.-Y. Choi, L. M. H. Hall and C. van de Bruck, *Spectral Running and Non-Gaussianity from Slow-Roll Inflation in Generalised Two-Field Models*, *JCAP* **0702** (2007) 029, [[astro-ph/0701247](#)].
- [38] M. Sasaki, *Multi-brid inflation and non-Gaussianity*, *Prog. Theor. Phys.* **120** (2008) 159–174, [[0805.0974](#)].
- [39] J. Meyers and N. Sivanandam, *Non-Gaussianities in Multifield Inflation: Superhorizon Evolution, Adiabaticity, and the Fate of fNL*, *Phys. Rev.* **D83** (2011) 103517, [[1011.4934](#)].
- [40] J. Elliston, D. J. Mulryne, D. Seery and R. Tavakol, *Evolution of fNL to the adiabatic limit*, *JCAP* **1111** (2011) 005, [[1106.2153](#)].

- [41] T. Faulkner, M. Tegmark, E. F. Bunn and Y. Mao, *Constraining  $f(R)$  Gravity as a Scalar Tensor Theory*, *Phys. Rev.* **D76** (2007) 063505, [[astro-ph/0612569](#)].
- [42] Y. Watanabe and E. Komatsu, *Reheating of the universe after inflation with  $f(\phi)R$  gravity*, *Phys. Rev.* **D75** (2007) 061301, [[gr-qc/0612120](#)].
- [43] S. Yokoyama, T. Suyama and T. Tanaka, *Primordial Non-Gaussianity in Multi-Scalar Inflation*, *Phys. Rev.* **D77** (2008) 083511, [[0711.2920](#)].
- [44] Y. Watanabe,  *$\delta N$  versus covariant perturbative approach to non-Gaussianity outside the horizon in multifield inflation*, *Phys. Rev.* **D85** (2012) 103505, [[1110.2462](#)].
- [45] X. Calmet and I. Kuntz, *Higgs Starobinsky Inflation*, *Eur. Phys. J.* **C76** (2016) 289, [[1605.02236](#)].
- [46] T. d. P. Netto, A. M. Pelinson, I. L. Shapiro and A. A. Starobinsky, *From stable to unstable anomaly-induced inflation*, *Eur. Phys. J.* **C76** (2016) 544, [[1509.08882](#)].